

UNIVERSITY OF NAPLES “FEDERICO II”



Department of Chemical, Material and Industrial Production
Engineering

PhD in Materials and Structures Engineering (XXVIII cycle)

Intumescent flame retarded polypropylene systems containing
sepiolite clays: properties and synergic effects

PhD supervisors

Prof. Giuseppe Mensitieri

Prof. Domenico Acierno

Eng. Pietro Russo

Candidate

Salvatore Pappalardo

INTRODUCTION	3
CHAPTER 1: FLAME RETARDANCY AND FIRE TEST.....	6
1.1. Flame retardancy of polymers	6
1.2. Role of fire tests	11
CHAPTER 2: FLAME RETARDANTS	13
2.1. Flame retardants.....	13
2.1.1. Mineral flame retardants.....	14
2.1.2. Halogenated compounds	15
2.1.3. Phosphorus-based flame retardants.....	18
2.1.4. Nitrogen-based flame retardants	19
2.1.5. Intumescent systems.....	20
2.1.6. Silicon-based flame retardants.....	21
2.1.7. Nanometric particles	21
CHAPTER 3: COMPOUNDING AND CHARACTERIZATION.....	25
3.1. Materials	25
3.2. Melt processing.....	25
3.3. Characterization	27
3.3.1. Thermal analysis	27
3.3.2. Flammability test.....	27
3.3.3. Fire behavior	30
3.3.4. Mechanical testing	32
3.3.5. Dynamic mechanical analysis (DMA)	32
3.3.6. Rheological analysis.....	33
3.3.7. Scanning electron microscopy (SEM).....	35
3.3.8. Transmission electron microscopy (TEM).....	35
CHAPTER 4: RESULTS AND DISCUSSION.....	36
4.1. Thermal stability	36
4.1.1. SEP and OSEP	36
4.1.2. First set of materials	37
4.1.3. Second set of materials.....	38
4.2. DSC analysis.....	42
4.2.1. First set of materials	42
4.2.2. Second set of materials.....	42
4.3. Flammability and ignitability	43
4.3.1. First set of materials	43

4.3.2. Second set of materials.....	44
4.4. Fire behavior.....	45
4.4.1. First set of materials.....	46
4.4.2. Second set of materials.....	48
4.5. Mechanical properties.....	51
4.5.1. First set of materials.....	51
4.5.2. Second set of materials.....	52
4.6. Dynamic mechanical analysis (DMA).....	54
4.6.1. First set of materials.....	54
4.6.2. Second set of materials.....	56
4.7. Rheological behavior.....	57
4.7.1. First set of materials.....	57
4.7.2. Second set of materials.....	58
4.8. Morphology of composites.....	61
4.8.1. First set of materials.....	61
4.8.2. Second set of materials.....	62
4.9. Conclusions.....	68

INTRODUCTION

Since the second half of the 20th century, plastics have become one of the most universally-used and multipurpose materials in the global economy. Today, plastics are utilized in more and more applications and they have become essential to our modern economy (Fig. 1).

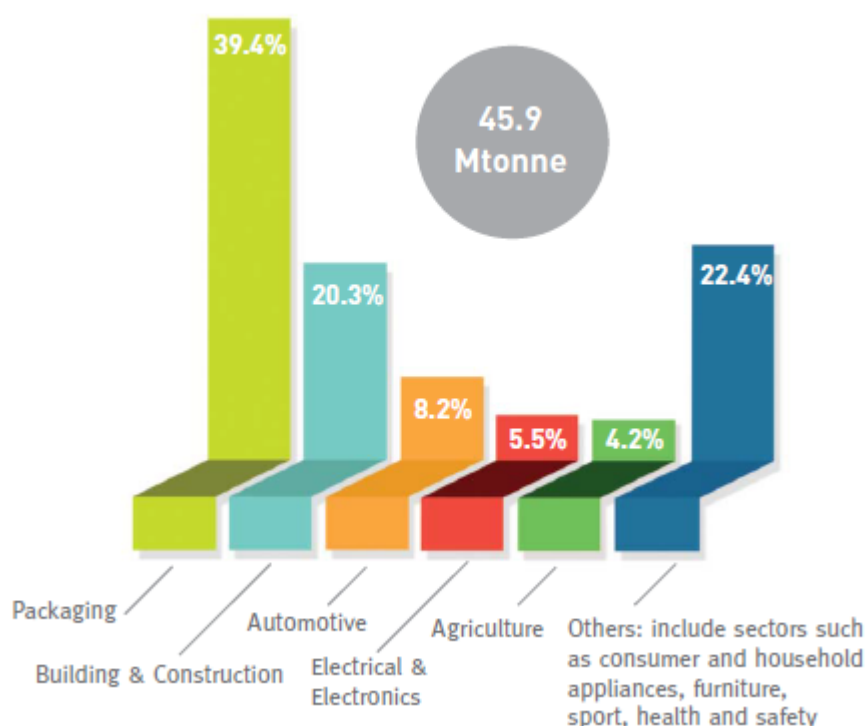


Figure 1. European plastics demand in 2012.

Polypropylene (PP) is one of the most commonly used thermoplastics. It has been widely used in many application sectors including packaging, automotive components, furniture, electronics etc. Main reasons of such success are the good mechanical properties, the easy processability and, last but not least, the relatively low price. The continuous improvements of synthetic routes, e.g. the use of better catalysts, have expanded the market of PP. Additional benefits have been achieved in terms of transparency and impact resistance at low temperatures through copolymerization with ethylene.

However, the aliphatic structure makes PP highly flammable, limiting the range of applications. Consequently great efforts have been spent to overcome this drawback by

using flame retardant agents. Among these latter, the flame-retardant properties of PP. Halogen-containing flame retardants are the most effective but their use has been strongly limited due to safety considerations and environmental concerns; in fact, they may release toxic and corrosive molecules. Metal hydroxides, such as aluminum hydroxide and magnesium hydroxide, are another kind of flame retardant additives in polyolefines. However, their yield of action is significantly lower than bromine-containing additives. Taking into account that, to achieve an adequate flame retardant effect, the content of these additives is usually higher than 30 wt%, the result is a considerable worsening of mechanical and rheological properties. The most effective way to improve the fire retardancy of PP is adding an **intumescent flame retardant (IFR)**, thanks to the very low smoke and toxic gases production and anti-dripping property. This kind of substance involves three components: an acid source, a carbonization agent (or char forming agent) and a blowing agent. Among these flame retardants, ammonium polyphosphate (APP)/pentaerythritol (PER)/melamine (MEL) systems are widely studied. The flame retardancy process of IFRs occurs according the following steps:

- the carbonization agent dehydrates to form melted char precursor under the catalysis of the acid substance
- the blowing agent, because of the high temperature, releases inert gases and expands the melted char precursor to create a swollen char layer. This swollen char layer can provide a barrier effect which avoids the direct contact between the polymer and the surrounding environment. The result is a reduced or cancelled transfer of oxygen and heat between the flame zone and the underlying material.

However, traditional IFRs have some drawbacks, such as a not outstanding efficiency, pretty low thermal stability and water resistance. To overcome these problems, a lot of research work has been done. For example, the addition of “**synergistic agents**” may enhance the efficiency of the flame retardants. The most common ones are zeolites [1,2], organoboron siloxane [3,4], and some transitional metal oxides and metal compounds [5-7]. Many researchers have shown that synergistic agents may increase the strength and stability of char layers.

In recent years it has been shown that pristine or organically modified sepiolite have synergistic flame retardant effects with in polypropylene based compounds [8,9].

This research work is focused on reducing flammability of PP by the use of different kinds of intumescent flame retardants coupled with sepiolite, either pristine or organically modified. The aim was to find the best compromise between flame retardancy and filler content. Moreover, a great importance was given to the study of the rheological and mechanical properties of the obtained formulations. The flammability and thermal stability of all the composites were examined by thermogravimetric analysis (TGA), and small flame tests (UL-94, LOI). The fire properties were studied by using forced-flaming conditions (cone calorimeter). Mechanical, dynamic-mechanical and rheological properties were also determined as a function of the filler content. Finally, SEM analysis was carried out to relate detected performances for all the investigated materials with the actual dispersion of included fillers.

CHAPTER 1: FLAME RETARDANCY AND FIRE TEST

1.1. Flame retardancy of polymers

The thermal decomposition of a polymer is an endothermic event, which requires an input of energy. The energy provided must be higher than the binding energy between the linked atoms (200 to 400 kJ/mol for most C-C polymers). The decomposition mechanism depends on the weakest bonds and the presence or absence of oxygen in the solid and gas phases. It is possible to distinguish between non-oxidizing and oxidizing thermal degradation [10]. Non-oxidizing thermal degradation is initiated by chain scissions under the effect of temperature (pyrolysis) and may occur in two ways:

- formation of free-radicals, which can start a chain reaction
- migration of hydrogen atoms and formation of two molecules, one of which has a reactive double bond

In oxidizing conditions, the polymer reacts with oxygen in the air and generates several products: carboxylic acids, alcohols, ketones, etc. This degradation also releases very reactive species (H^{\bullet} and OH^{\bullet}), particularly in polyolefines. The propagation rate of the decomposition process is controlled by the wrenching reaction of hydrogen atoms from the polymer chains. The oxidation stability of the polymer thus depends on the C-H bond energy.

The flammability of a material is not an intrinsic property, like its density or heat capacity, but is dependent on the fire conditions. The fire triangle shown in Fig. 2, useful to demonstrate the dependence of the material properties with heat and ventilation, shows where flame retardants can interfere in the combustion process. Generally, fire growth is more favorable if the heat flux or oxygen supply increases. However, excessive ventilation may remove heat from the fire, while additional heat may also lead to melting or char formation, followed by a reduced fire growth.

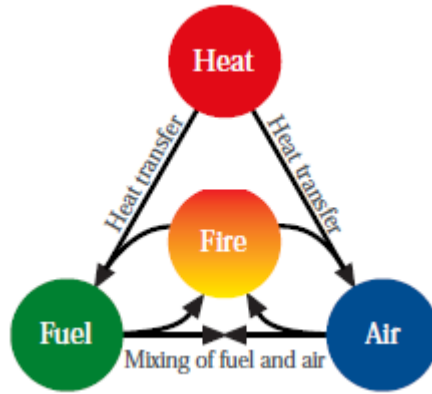


Figure 2. The fire triangle.

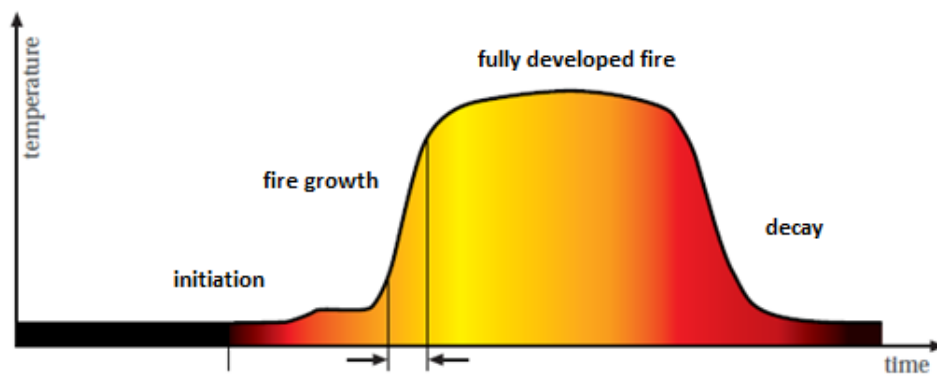


Figure 3. Different stages of combustion process.

A fire may be split into three phases: ignition, fully developed fire and decreasing fire (Fig. 3). During the ignition phase (Fig. 4), the increase in temperature may reach a value high enough to break the chemical bonds and produce volatile fragments. Once a sufficient concentration is reached, these fragments can lead to a stable flame. The ignition may also be due to an external source (e.g. match or cigarette).

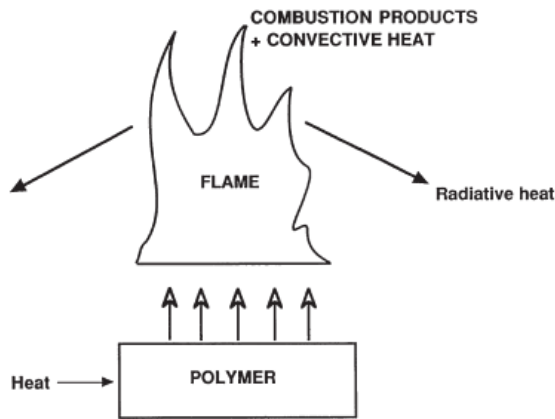


Figure 4. Ignition process.

The heat transfer processes are critical to the ignition and fire behavior. Once ignited, the fire initially grows by a process of flame spread: the surfaces next to the flame zone decompose to form more flammable products, so flame spread is basically a process of repeated ignitions.

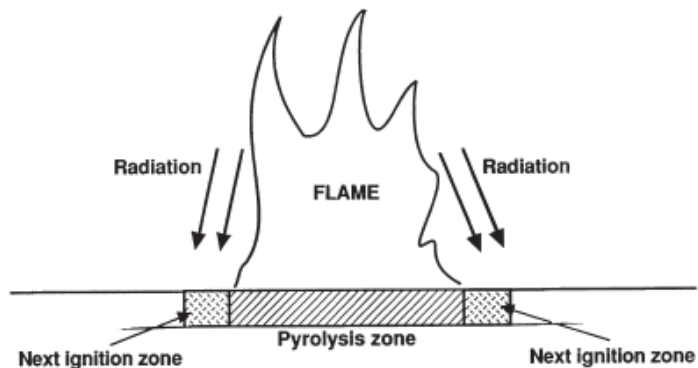


Figure 5. Horizontal flame spread.

Horizontal flame spread (Fig. 5) is slow because the material near the flame is heated by gas-phase conduction and downward radiation. Upward flame spread is faster, because radiative, convective and some conductive heat transfer occur (Fig. 6).

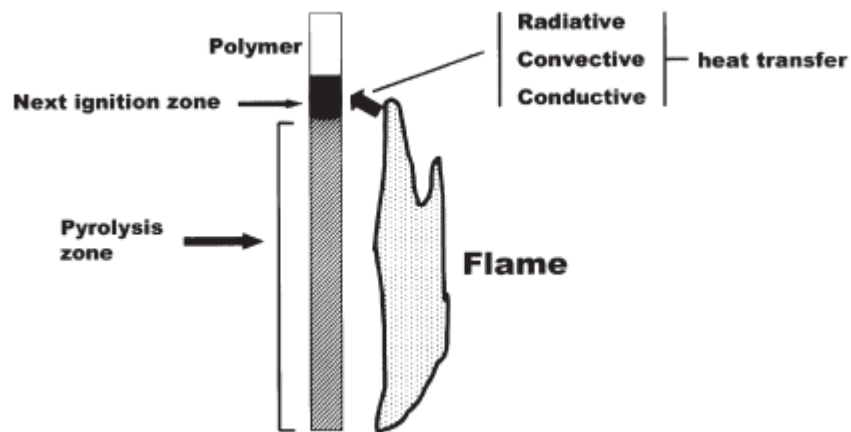


Figure 6. Vertical flame spread.

Conductive and convective transfers are very important in the ignition phase, when the height of the flame is limited to few centimeters. In a more advanced phase, flame propagation on the surface contributes to a rapid increase in radiative transfer. The fire spreads, heats up the surroundings and, once the materials in the room have formed enough flammable gases and are sufficiently hot, flashover takes place and the whole room is engulfed in the fire. This is the start of the fully developed fire, where temperatures up to 1200°C may be reached. Then the fire decreases because the available fire load is consumed or there is an oxygen deficiency.

Flame retardants (Fig. 7) can inhibit or even suppress the combustion process by chemical and/or physical actions [11,12]. They interfere with combustion during a particular stage of this process, e.g. heating, decomposition, ignition or flame spread. The amount of flame retardant required depends on the material and the desired level of fire safety: it may range from 1 up to 50 wt% but usually the typical range is 5-20 wt%. The chemical action is usually more effective than the physical one and takes place in several ways:

- **reaction in the gas phase:** the radical reactions of the flame can be interrupted by a flame retardant, so the system cools down. However, this interferes with the flame reactions and results in toxic and irritant products, including CO, which generally increase the toxicity of the fire
- **reaction in the solid phase:** the flame retardants work by breaking down the polymer chains so the melt material flows away from the flame. The drawback is the production of flammable drops, not allowing a good fire safety level

- **char formation:** high temperature leads to a layer of carbonaceous char on the polymer surface, that, among other, reduces the formation of smoke and other products of incomplete combustion
- **intumescence:** the incorporation of blowing agents causes swelling behind the surface layer and provides better insulation under the protective barrier.

The physical action may take place by three different mechanisms:

- **cooling:** absorption of energy triggered by additives and/or the chemical release of water cools the substrate to a temperature below that required for sustaining the combustion process
- **formation of a protective layer:** preventing heat and oxygen exchange between the material and the heat source
- **dilution:** inert substances and additives dilute the fuel in the solid and gaseous phases.

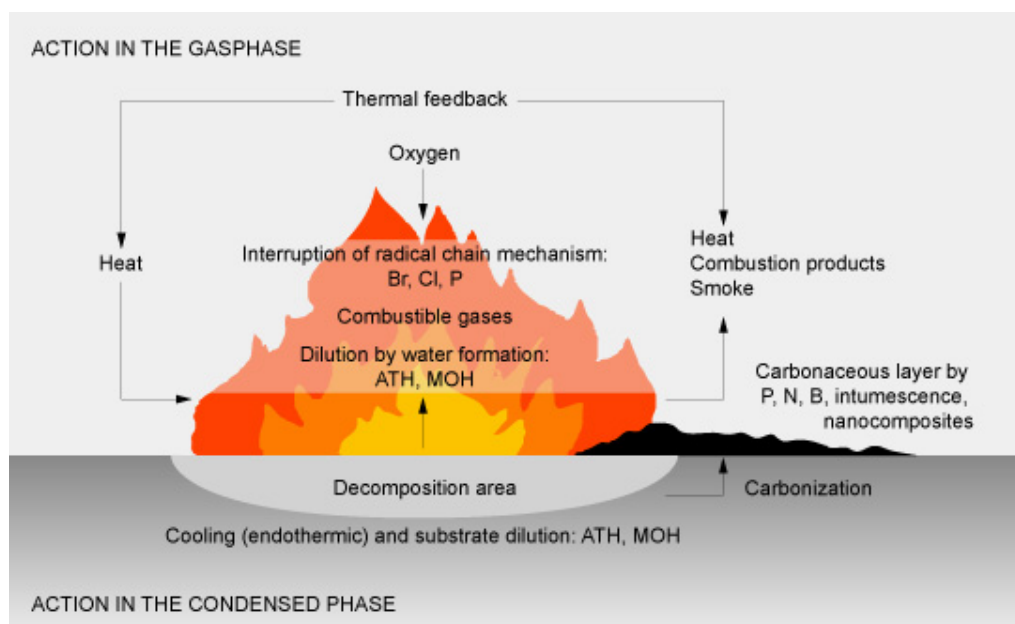


Figure 7. Action of flame retardants.

1.2. Role of fire tests

Fire tests are used to determine the fire risk of materials and products used in applications like building, electrical equipment and furniture. This kind of test is developed to simulate the ignition behavior of materials or real fire events. To simulate the effects of fire, the test conditions should be related to the appropriate scenario:

- **ignition:** the obtainment of repeatable results from spontaneous ignition is difficult but it is the only way to assess the onset of flaming combustion
- **developing fire:** the fire growth involves an external heat flux of around 20- 60 kW m⁻², which requires larger specimens, temperatures above the ignition temperature (400-600°C) and adequate ventilation
- **fully developed fire:** it involves high external heat fluxes (450 kW m⁻²), large sample sizes, high temperatures and low ventilation. These conditions are not easy to replicate on a small scale and materials which have to perform adequately need to be tested under these extreme conditions

The products have to satisfy fire safety requirements defined in the tests. The sample size can vary from a small piece of material (e.g. 127x13x3 mm³ for the UL-94 test) up to boards of 1.5x1.5 m² (SBI-test), individual furniture items or even complete furnished rooms. Analysis of fire statistics shows that most fire deaths are caused by inhalation of toxic gases [13]. Burning behavior and toxic products yields mainly depend on material composition, temperature and oxygen concentration. The formation of carbon monoxide, often considered the most toxicologically significant fire gas, is favored by some conditions, e.g. smouldering or fully developed flaming. Incomplete combustion phenomena give rise to CO production for many reasons as

- insufficient heat in the gas phase
- quenching of the flame reactions
- presence of stable molecules, which survive long time in the flame zone, give high CO yields in well-ventilated conditions, but low yields in under-ventilated [14] and insufficient oxygen conditions.

The high yields of CO from under-ventilated fires are responsible for most of the deaths through inhalation of smoke. Another toxic species is the hydrogen cyanide (HCN) which can inhibit breathing and prevent escape. Data from large-scale fires [15,16] show very high levels of CO and HCN under conditions of reduced ventilation. Another dangerous aspect is related to the possible presence of molecules such as dioxins and polycyclic aromatic hydrocarbons. Although they don't cause an immediate danger, they may induce long-term damage to human health and environment. However, compared to the toxic potential of CO, all the other fire gas components play a minor role.

CHAPTER 2: FLAME RETARDANTS

2.1. Flame retardants

The worldwide consumption of flame retardants amounts to around **2 million tons a year**. The use of flame retardants has grown substantially in past years, particularly in electronics, and will continue to grow at a global rate of 5%. The ever more widespread use of plastics accounts for approximately 85% of all flame retardants used with textiles and rubber products accounting for most of the rest.

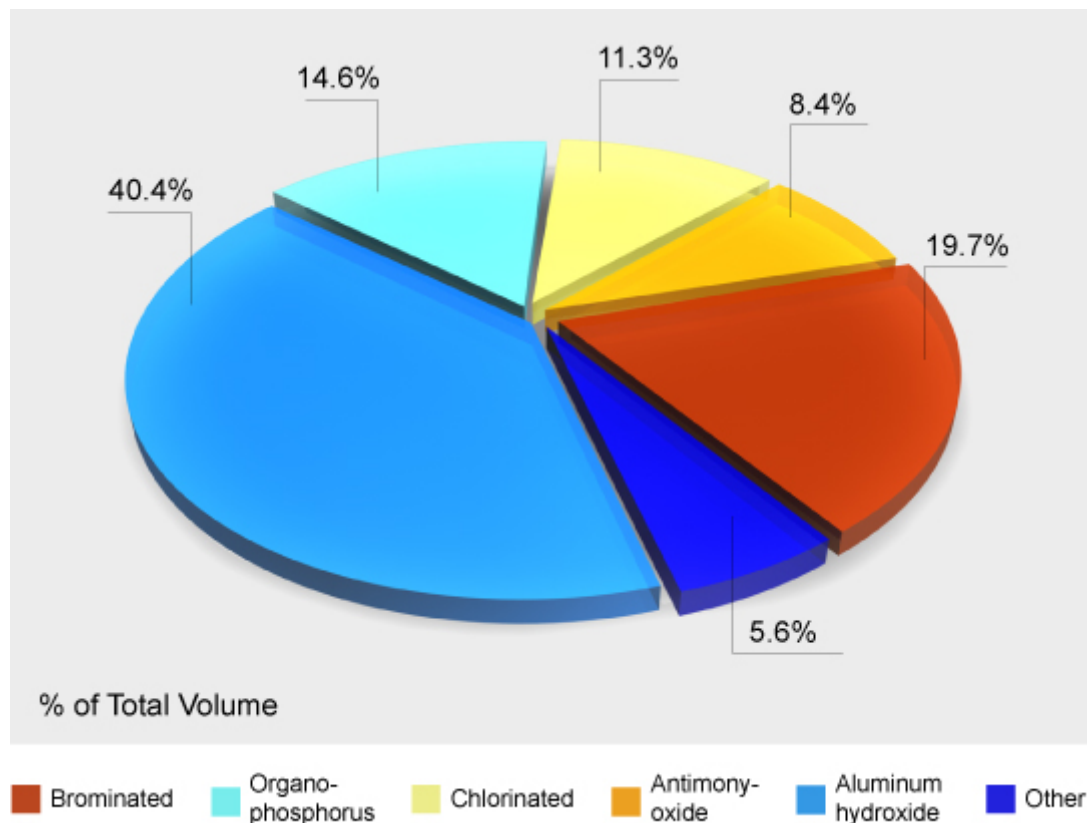


Figure 8. Worldwide consumption of flame retardants.

Asia-Pacific is the largest sales market for flame retardants and China accounts for 24% of global demand. North America continues to be the second largest market, followed by Western Europe. The most important application area for flame retardants is the construction sector. A considerable amount of flammable materials is used in thermal insulation and improvement of energy efficiency of residential buildings. Pipes and cables made of plastics are both used in the construction of new buildings and the

refurbishment of old ones, and are increasingly replacing conventional products such as pipes made of metal. The transportation industry (vehicles and aerospace) also requires high-performance flame retardants. In the future, electrics and electronics will be the largest growth market. In particular, manufacturers of smartphones and tablet computers will raise demand for flame retardants and put a rising value on the environmental impact of these substances.

There are several kinds of flame retardants, which have different chemical structure:

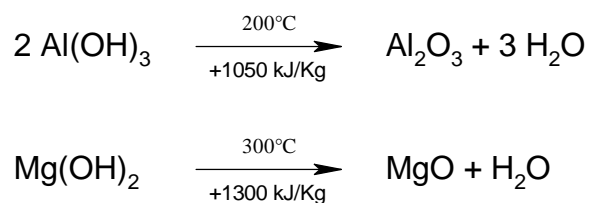
- minerals (based on aluminum and magnesium hydroxides)
- halogens (bromine and chlorine)
- P and N based-substances
- intumescent systems
- others (sodium borate, Sb_2O_3 , nanocomposites etc.).

2.1.1. Mineral flame retardants

Inorganic fillers can influence the fire properties of polymers:

- reducing the content of combustible products
- modifying the thermal conductivity of the material and its thermal properties
- changing the viscosity of the resulting material.

Some minerals are more specifically used as flame retardants thanks to their behavior at high temperature. Aluminum trihydroxide (**ATH**) is by far the most widely used flame retardant on a tonnage basis. It is cheap but requires high loadings in polymers up to 60 wt% [17,18]. The flame retardant mechanism is based on the release of water which cools and dilutes the gases feeding flames, absorption of heat and formation of a protective layer on the surface. Magnesium hydroxide (**MDH**) acts as ATH and is used in polymers which have higher processing temperatures, because it is stable up to temperatures of around 300°C (ATH decomposes at 200 °C).



ATH and MDH powders are used in melt compounding and extrusion of thermoplastics like PVC or polyolefines.

Recently MDH and ATH nanoparticles have been considered as flame retardants. They may be obtained by several methods: sol–gel technique followed by a hypercritical drying procedure [19], a hydrothermal reaction using various precursors and solvents [20] or by precipitation of magnesium salts with an alkaline solution [21]. The use of nanometric MDH can enable interesting fire performances at lower loading levels. It has been shown [22] that the LOI obtained with EVA containing MDH 50 wt% increases from 24% to 38% when the additive is nanometric. The enhancement was attributed to the excellent dispersion of the nanoparticles, which leads to the formation of more compact and cohesive char during the combustion test.

Borates are another family of inorganic flame retardants. Among them, zinc borate is the most used and is suitable for PVC and other plastics like polyolefines, elastomers and polyamides. Their endothermic decomposition between 290 and 450°C releases water, boric acid and B₂O₃, that leads to the formation of a protective vitreous layer. In the case of polymers containing oxygen atoms, the presence of boric acid causes dehydration, leading to the formation of a carbonized layer. This layer prevents the heat and oxygen exchange between polymer and surrounding.

2.1.2. Halogenated compounds

The efficiency of halogenated flame retardants depends on the type of halogen. Fluorine and iodine-based compounds are not used because they do not interfere with the polymer combustion process. Fluorinated compounds are more thermally stable than most polymers and do not release halogen radicals at the decomposition temperatures of the polymers [23]. Iodinated compounds are less thermally stable than most commercial polymers and therefore release halogenated species during polymer processing. That explains why only brominated and chlorinated substances are used as flame retardants.

There are more than 50 commercial brominated flame retardants (**BRFs**). The only common characteristic is that they contain bromine and act in the gas phase by a radical trap mechanism, inhibiting the formation of flammable gases.

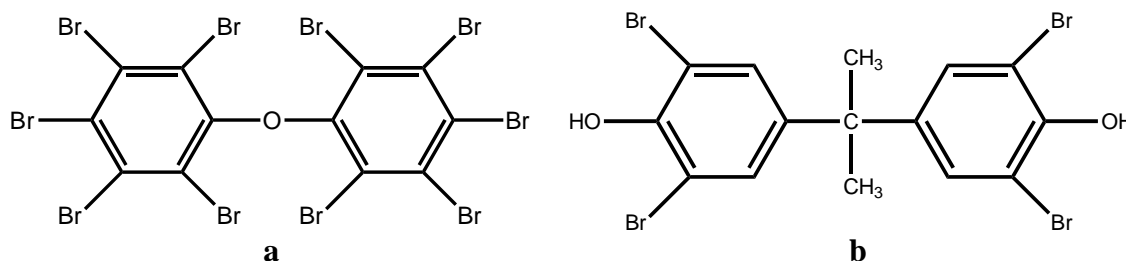


Figure 9. Deca-BDE (a) and TBBPA (b).

Decabromodiphenylether (Deca-BDE, Fig. 9) is a universally used flame retardant for plastics and textiles. It has got 10 bromine atoms bonded to the diphenylether molecule and possesses high molecular weight and great thermal stability. Its major applications are in polyolefines, polyesters, nylons and textiles. However, in Europe its use is partially banned and in US the production will be stopped soon. Tetrabromobisphenol-A (TBBPA) is mainly used in epoxy resins for printed wiring boards.

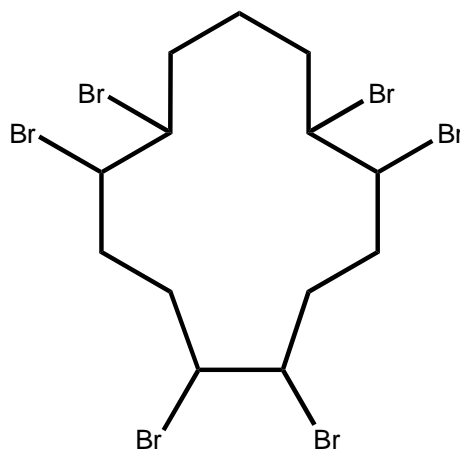


Figure 10. Chemical structure of HBCDD.

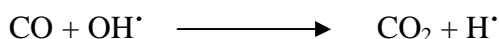
Hexabromocyclododecane (HBCDD, Fig. 10) is a cycloaliphatic BFR. It is commonly used in foamed polystyrene for insulation of buildings.

With regard to the mechanism, the halogenated substances can produce halides by thermal degradation in the condensed phase or in the gas phase. These molecules can interrupt the process of combustion, indeed they can neutralize H[•] and OH[•] radicals and

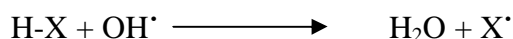
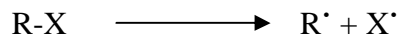
inhibit the radical chain mechanism that takes place in the flame. Oxygen is consumed by reaction with H^\cdot : this reaction has a very important effect on the kinetics of combustion.



The reaction between CO and OH^\cdot is instead strongly exothermic and supplies a large amount of heat.



At first, the flame retardant breaks up and produces halogen and aliphatic radicals. Then, the halogen radicals react to form hydrogen halide, which interferes with the radical chain mechanism. The high energy H^\cdot and OH^\cdot radicals are removed by reaction with HX and replaced with low energy X^\cdot radicals. The hydrogen halide is regenerated by reaction with hydrocarbon, thus HX acts a catalyst.



Since halogenated flame retardants are regenerative, much lower loadings (about 10 wt%) are required compared to ATH or MDH (typically 50 wt%). Brominated flame retardants are more effective than those containing chlorine because of a narrow range of vaporization temperature, leading to higher concentration of the flame retardant in the flame zone. Synergistic agents, such as antimony oxides, further increase the effectiveness of both brominated and chlorinated flame retardants by enabling the halogen to stay in the flame zone for longer periods.

Use of halogenated compounds has given rise to some concern: a lot of attention has been focused on the corrosiveness and toxicity of smoke generated during the

combustion of plastics utilizing these materials. In contrast to the hazardous halogenated flame retardants, MDH and ATH are much less problematic. Additionally, as landfill space declines or becomes unpopular, incineration and recycling of used plastics will become more widespread. Plastics formulated with halogenated flame retardants create problems for incinerators in design, operation and maintenance, as well as a danger to public health from the incineration product gases

2.1.3. Phosphorus-based flame retardants

The class of phosphorus-containing flame retardants covers a wide range of inorganic and organic compounds. They have a broad application field and good fire safety performance. The most important phosphorus-containing flame retardants are the following:

- red phosphorus,
- ammonium polyphosphate (**APP**),
- phosphate esters, phosphonates and phosphinates.

Phosphorous-containing FRs mainly act in the solid phase of the polymer. They are very effective in materials containing a high amount of oxygen [24,25]. By thermal degradation, the FR decomposes to phosphoric acid which esterifies and extracts water from the polymeric matrix. This leads to the formation of char, a complex network of carbon and phosphorous oxides. Specific phosphorus-containing flame retardants such as metal phosphinates may also act in the gas phase by the formation of P^{\cdot} , PO^{\cdot} and PO_2^{\cdot} radicals interrupting the radical chain mechanism of the combustion process. Phosphorous-containing FRs have very good performances and don't release toxic smoke, however their weaknesses are the high cost and the potential corrosiveness of the combustion products.

Flame retardants based on red phosphorus are mainly used in polyamide 6 and 66: they can meet UL-94 V-0 level at low dosages and are particularly effective in glass fiber reinforced formulations [26]. However, red phosphorus has a big disadvantage: it may release highly toxic phosphine (PH_3) through reaction with moisture.

Ammonium polyphosphate (APP) is an inorganic salt derived from polyphosphoric acid and ammonia and characterized by variable chain length: short chain APPs ($n < 100$) are

more water sensitive and less thermally stable than longer chain APPs ($n > 1000$). It is well known that the incorporation of APP in polymers containing O and N (polyesters, polyamides, polyurethanes) leads to charring, so it is very effective even at low concentration [27-29]. Moreover, APP is used in intumescent coatings for polyolefines. Phosphate esters are used as flame retardants in PVC, engineering plastics (particularly in polyphenylene oxide/high impact polystyrene (PPO/HIPS), PC/ABS blends [30,31]. Phosphonates and phosphinates (Fig. 11) are used as flame retardants in flexible polyurethane foams for automotive and building applications [32].

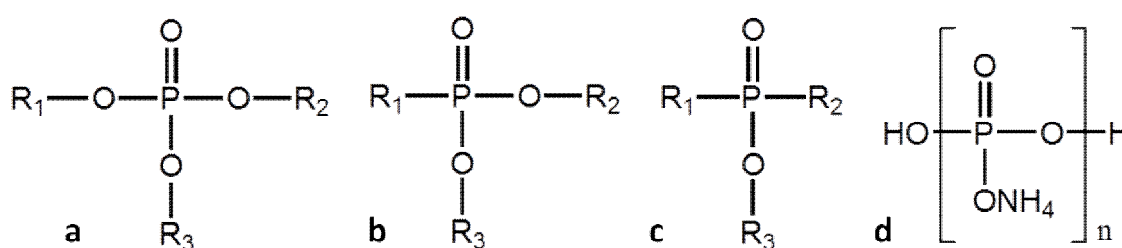


Figure 11. Phosphate esters (a), phosphonates (b), phosphinates (c) and APP (d).

2.1.4. Nitrogen-based flame retardants

There are three kinds of nitrogen-based FRs:

- pure melamine,
- melamine derivatives (salts with organic or inorganic acids such as boric acid and phosphoric acid), and
- melamine homologue.

This kind of molecules act by several mechanisms: in the condensed phase, melamine is transformed into cross-linked structures which promote char formation. Ammonia is released in these reactions. In the gas phase the release of molecular nitrogen dilutes the volatile polymer decomposition products [33].

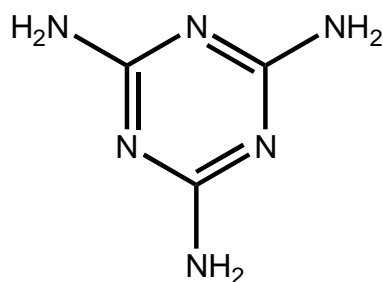


Figure 12. Melamine.

Melamine (Fig. 12) is mostly used in polyurethane foams, whereas melamine cyanurate is used in nylons or in polypropylene intumescent formulations in conjunction with ammonium polyphosphate. The drawbacks are related to the high concentration necessary to obtain good fire performance and the mechanism, not fully understood yet.

2.1.5. Intumescent systems

Intumescent flame retardant systems expand to produce foams. They are used as coatings to protect combustible materials such as wood and plastics, but also steel based structures in buildings.

The intumescent effect is achieved by combining an acid source like ammonium polyphosphate (**APP**), a source of carbon which releases non-combustible gases, and a blowing agent. At high temperatures, APP decomposes releasing acid species that catalyze the dehydration reaction of the carbonizing agent, leading to the formation of a carbonaceous layer. The acid has to be liberated at a temperature below the decomposition temperature of the carbonizing agent and its dehydration should occur at the decomposition temperature of the polymer. The carbonizing agent is generally a carbohydrate that produces char during thermal decomposition. Its effectiveness is related to the number of carbon atoms and reactive hydroxyl sites. The amount of char produced during thermal decomposition is highly dependent on the number of carbon atoms, whereas the number of reactive hydroxyl sites determines the rate of the dehydration reaction and thus the rate of formation of the carbonized structure. The blowing agent, usually a melamine derivative, releases water and nitrogen which create a foam that expands to form an insulating char barrier (Fig. 13).

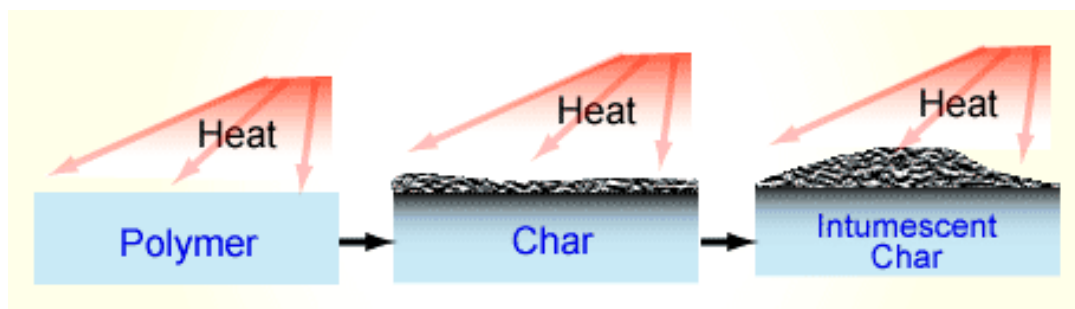


Figure 13. Protection mechanism of intumescent.

2.1.6. Silicon-based flame retardants

Adding low amounts of silicon-based compounds (silicones, silica, organosilanes, silsesquioxanes and silicates) to polymers can substantially improve their flame retardancy [34]. They may be used as fillers incorporated in the polymer or as copolymers. Silicones have excellent thermal stability and release very low amounts of toxic gases during thermal decomposition. They are usually used in PC (polycarbonate) based compounds because of the reaction mechanism: Zhou suggested that the hydroxyl groups present in PC degradation products could react with the carbon-silicon bond yielding a cross linked structure and a condensed aromatic structure [35]. Silica gel can enhance the flammability properties of polypropylene [36]. Calorimeter tests revealed a significant reduction of the HRR (heat release rate) of PP containing 10 wt% porous silica. Authors explained this effect by the possibility offered by larger pores to accommodate macromolecular PP chains or by the increase of molten viscosity during pyrolysis, which can trap or slow down volatilization and the development of degradation products.

2.1.7. Nanometric particles

Nanometric fillers, if well dispersed in polymer matrices, can enhance thermal, mechanical or fire resistance properties even at low amounts. The large increase of interfacial area between the polymer and the nanofillers is the key factor to explain the exceptional properties of the nanocomposites. With regard to flame retardancy, it may vary and strictly depends on the chemical structure and geometry. There are three kinds of largely used nanofillers:

- **layered materials**, such as nanoclays (e.g., montmorillonite), characterized by one nanometric dimension
- **fibrous materials**, such as carbon nanotubes and sepiolite, characterized by elongated structures with two nanometric dimensions
- **particulate materials**, e.g. polyhedral oligosilsesquioxane (POSS) and spherical silica nanoparticles, characterized by three nanometric dimensions.

Nanoclays can work as flame retardant owing to the formation of char and reassembling of the silicate layers, which generates a ceramic structure at the material surface. Moreover they can increase melt viscosity of hosting polymeric materials by exfoliating. These mechanisms modify the fire properties of the polymer nanocomposite, sometimes improving them and in some other cases worsening them. For example the incorporation of nanoclays generally retards and decreases the peak heat release rate, but does not reduce the total heat involved. The char formed at the surface of the burning sample during UL-94 and LOI tests usually is not enough to stop the flame and the sample continues to burn slowly. In order to favor the dispersion of the nanoclays within the polymer, a modification of natural clays using organic cations is often carried out, leading to the formation of organomodified nanoclays [37,38].

Carbon nanotubes possess exceptional properties that may be used in many applications ranging from macroscopic material composites to nanodevices. Thanks to their high aspect ratio, CNTs percolate to form a network in the polymer matrix and lead to substantial enhancement of mechanical [39], rheological [40-42] and flame retardant [43-45] properties. With regard to the fire properties, it has been observed that the incorporation of very small amounts of CNTs (from 0.5 to 4 wt%) can lead to a marked decrease of HRR. Based on some observations, the flame retardant properties of these nanocomposites are governed by two physical processes: the structured layer acts as a shield and re-emits part of the incident radiation back into the gas phase, decreasing the polymer degradation rate. On the other hand, the carbon nanotubes increase the thermal conductivity of the polymer so the PHRR (peak heat release rate) increases with the CNTs content. It means that a balance between thermal conductivity and shielding effects must be obtained.

Sepiolite is a hydrated magnesium silicate with formula $\text{Si}_{12}\text{O}_{30}\text{Mg}_8(\text{OH})_4(\text{H}_2\text{O})_4 \cdot 8\text{H}_2\text{O}$. Unlike other clays, it is not a layered phyllosilicate. Its peculiar structure (Fig.

14) is formed by two layers of silica tetrahedrons linked by a layer of magnesium ions in octahedral coordination. The octahedral sheets are not continuous and form long channels along the fiber direction [46–50].

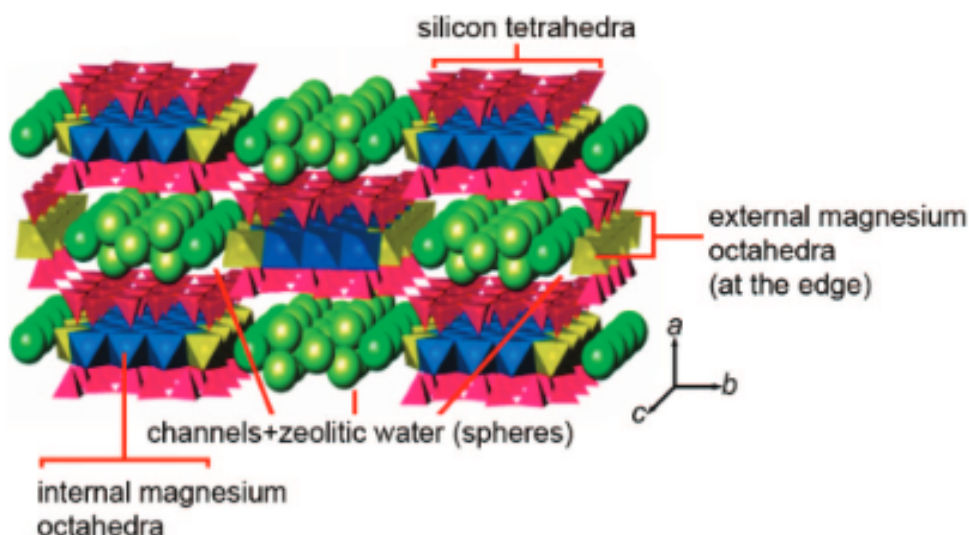


Figure 14. Structure of sepiolite.

These nanoscale tunnels are normally filled with water and measure approximately $3.5 \times 10.6 \text{ \AA}^2$ in cross section and 3 \mu m in length. The presence of such tunnels explains the acicular morphology of sepiolite and the very high surface area. The result is a good compatibility with most polymers and an increase of mechanical properties [51-57]. It has been showed that sepiolite may enhance the thermal stability and fire properties of PP/IFR composites [58]. He and coworkers, instead, showed that modified sepiolite may improve the fire properties if coupled with zinc borate as flame retardant [59], also because of a better compatibility between the resin and the nanofiller.

Another family of additives consists of nanoparticles of metal oxides, silica and POSS. These nanoscale additives are characterized by their isometric dimensions and have very interesting properties with regard to flame retardancy [60-63]. POSS is an inorganic silica-like nanocage surrounded by eight organic groups that enhance its compatibility within organic polymers. During combustion, POSS acts as a precursor forming thermally stable ceramic materials. The wide range of organic groups available enables the selective use of functionalized POSS according to the chemical nature of the polymer matrix. The inclusion of nanometric metal oxides can also improve the fire properties of many polymers. Laachachi studied the effect of the incorporation of

nanometric titanium oxide (TiO_2) and ferric oxide (Fe_2O_3) particles on the thermal stability and fire reaction of PMMA. Small amount (5 wt%) of nanometric TiO_2 or Fe_2O_3 enhanced the thermal stability of PMMA nanocomposites. HRR values, determined by the cone calorimetry test, were found to depend on the filler content and to decrease at higher loadings. The improved flame retardancy of these nanocomposites was attributed to a restriction of the mobility of polymer chains resulting from strong interactions between them and the surface of nanoparticles. Furthermore it was shown that the flame retardant effect of both TiO_2 and Fe_2O_3 depends on their particle size and surface area.

The incorporation of nanoparticles reduces polymer flammability by several mechanisms (limiting fuel transfer to the flame, formation of a protective char layer, etc.). However these nanocomposites still burn with a little reduction in total heat release and time to ignition is generally not improved. In other words, nanoparticles have to be used in combination with other flame retardant agents in order to achieve the required fire performance levels.

CHAPTER 3: COMPOUNDING AND CHARACTERIZATION

3.1. Materials

PP resin (block copolymer propene-ethene, melt flow rate 25 g/10 min) used in this work was produced by Unipetrol under the trade name MA524. Two kinds of intumescent flame retardants were used: Exolit AP750 (ammonium polyphosphate as main component, P content of 22 wt%, N content of 13 wt%) and Exolit AP766 (ammonium polyphosphate as main component, P content of 24 wt%, N content of 15 wt%), both supplied by Clariant. Polybond 3200 (1 wt% of maleic anhydride) was produced by Additivant. From this point forward, Exolit AP750, Exolit AP766 and Polybond 3200 will be respectively coded as **EX**, **ET** and **PB 3200**. Sepiolite (**SEP**) was supplied by Sigma-Aldrich while the organically modified sepiolite (**OSEP**) was made with the following two step procedure [8]:

- 25 g sepiolite were poured in 240 ml of deionized water and mixed at room temperature. HCl was added in the system to obtain a pH value equal to 3-4. The resulting slurry was stirred for 5 hours at room temperature. Successively it was filtered using a Buchner funnel. Finally, the obtained material was dried overnight.
- 12 grams of acid sepiolite was mixed with 180 ml of deionized water at room temperature. A second mixture of 10 wt% CTAB (cetyltrimethylammonium bromide) was prepared and 5.7 ml of this was added to the first suspension. The mixture was stirred for 5 hours at 75 °C, then filtered using a Buchner funnel and dried overnight to obtain OSEP.

3.2. Melt processing

Melt processing is the most widely method used to process thermoplastics and to obtain composites based on them. In this work, all the formulations were first obtained by using a twin screw micro extruder (DSM Explore) and, successively, a larger twin screw extruder (HAAKE Polylab). PP MA524 and the flame retardants were used as received because they are not hygroscopic, SEP and OSEP were instead dried in a

vacuum oven at 80°C overnight. The quality of the extruded materials could be tuned by changing several parameters, e.g. temperature, mixing time and shear rate. With regard to the micro extruder, plenty of tests demonstrated that the best processing conditions were the following ones:

- temperature 185°C
- mixing time 4 minutes
- screw speed 70 rpm.

These conditions guaranteed a very good dispersion of the fillers inside the matrix, without the risk of decomposing the flame retardant. Similarly, the optimal parameters were used for the twin screw extruder: the temperature profile was in the range 160-200°C from the feed to the die section of the barrel and the screw speed was equal to 60 rpm. These conditions ensure a good dispersion of the additives inside the matrix and prevented degradation effects of the flame retardants, as confirmed by subsequent tests. Resulting materials were water cooled and pelletized with a rotary cutter mill. All the specimens were made by compression molding using a hydraulic press mod. LP420 by LabTech engineering Company Ltd.

The formulations shown in Tab. 1 represent the first set of materials, characterized at the laboratories of the University of Naples “Federico II”. The second set of materials, listed in Tab. 2, was mainly characterized at the BAM (Bundesanstalt für Materialforschung und –prüfung) located in Berlin.

Table 1.

The first set of materials (all the values are expressed as wt%).

Sample	PP MA 524	PB 3200	EX	SEP
PP	100	0	0	0
PP/1SEP	98	1	0	1
PP/18EX	82	0	18	0
PP/25EX	75	0	25	0
PP/18EX/1SEP	80	1	18	1

Table 2.

The second set of materials (all the values are expressed as wt%).

Sample	PP MA 524	PB 3200	ET	SEP	OSEP
PP	100	0	0	0	0
PP/0.5SEP	99	0.5	0	0.5	0
PP/0.5OSEP	99.5	0	0	0	0.5
PP/12ET	88	0	12	0	0
PP/15ET	85	0	15	0	0
PP/12ET/0.5SEP	87	0.5	12	0.5	0
PP/12ET/0.5OSEP	87.5	0	12	0	0.5

3.3. Characterization

3.3.1. Thermal analysis

With regard to SEP, OSEP and the first set of materials, the thermogravimetric analysis was carried out using a TA Instruments Q5000 (Mettler-Toledo, Germany). Measurements were conducted in the range 40-700°C at a heating rate of 20°C/min under a 25 mL/min nitrogen flow. The weight of the samples was kept under 10 mg.

With regard to the second set of materials, the analysis was carried out by using a TG 209 F1 (Netzsch, Germany) in the range 30-900°C at a heating rate of 10°C/min under nitrogen or synthetic air flow (30 mL/min).

The DSC analysis was carried out by a TA Instruments Q20 (Mettler-Toledo, Germany). The samples were encapsulated in Al pans and heated from room temperature to 200°C, kept isothermal for 2 minutes, cooled to 25°C and heated again to 200°C.

3.3.2. Flammability test

The test for flammability of plastic materials used for electronic devices and appliances is commonly known as UL-94: a flammability specification issued by the Underwriters Laboratories Inc. The UL-94 family contains 6 different flame tests divided into two categories, vertical and horizontal testing (Tab. 3). In the vertical flame test, a flame is applied to the base of the specimen held in vertical position and the extinguishing times are determined upon removal of the flame. In horizontal flame tests,

the flame is applied to the free end of specimens held in horizontal position and the rate of burning is determined as the flame front progresses between two benchmarks.

Table 3.

Different types of UL-94 tests.

Test	Specimen	Dimensions (mm)	Rating
Horizontal	2 sets of 3 specimen	125x13; max thick. 13	HB
Vertical	4 sets of 5 specimen	125x13; max thick. 13	V-0, V-1, V-2
Vertical bar or plaque	4 sets of 5 specimen	125x13; max thick. 13	5VA, 5VB
	4 sets of 3 plaques	150x150; max thick. 13	
Thin material vertical	4 sets of 5 specimen	200x50	VTM-0, VTM-1, VTM-2
Radiant panel	1 set of 4 specimen	460x150	RP15/RP200
Foamed horizontal	4 sets of 5 specimen	150x150; max thick. 13	HBF, HF-1, HF-2

In terms of usage, UL-94 V (**IEC 60695-11-10**) is the most commonly used test to get a preliminary indication of flammability of polymers: it measures the self-extinguishing time of a vertically oriented specimen. The top of the specimen is clamped to a stand and the burner is placed directly below the specimen (Fig. 15). In Tab. 4 there are all the possible outcomes for the UL-94 V test: the best ranking is represented by the V-0 level, the worst one by the V-2 level which involves the presence of flaming drippings, very risky in case of fire.

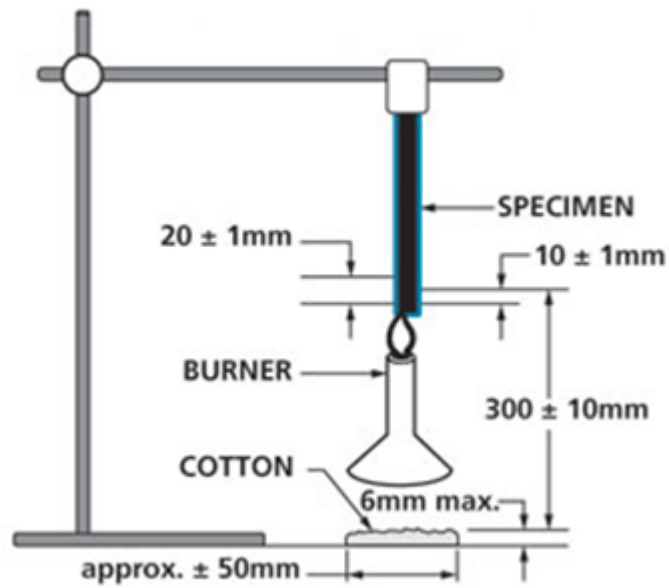


Figure 15. How the UL-94 test is carried out.

Table 4.

Possible ratings for UL-94 V tests.

V-0	Burning stops within 10 seconds after two applications of ten seconds each of a flame to a test bar. NO flaming drips are allowed.
V-1	Burning stops within 60 seconds after two applications of ten seconds each of a flame to a test bar. NO flaming drips are allowed
V-2	Burning stops within 60 seconds after two applications of ten seconds each of a flame to a test bar. Flaming drips are allowed

The LOI test (Fig. 16) is used to determine the minimum concentration of oxygen that supports flaming combustion. LOI data are obtained at room temperature according to **ISO 4589**. The dimension of the samples is 100x10x4 mm³. A specimen is positioned vertically in the test column and a mixture of oxygen and nitrogen is forced upward through the column. The specimen is ignited at the top. The oxygen concentration is adjusted until the specimen supports combustion. The index is expressed as follows:

$$LOI = 100 \frac{[O_2]}{[O_2] + [N_2]}$$

A material passes the test if its LOI value is higher than 21%, which represents the concentration of oxygen in the air. The higher this value is, the better the flame retardancy properties of the material are.

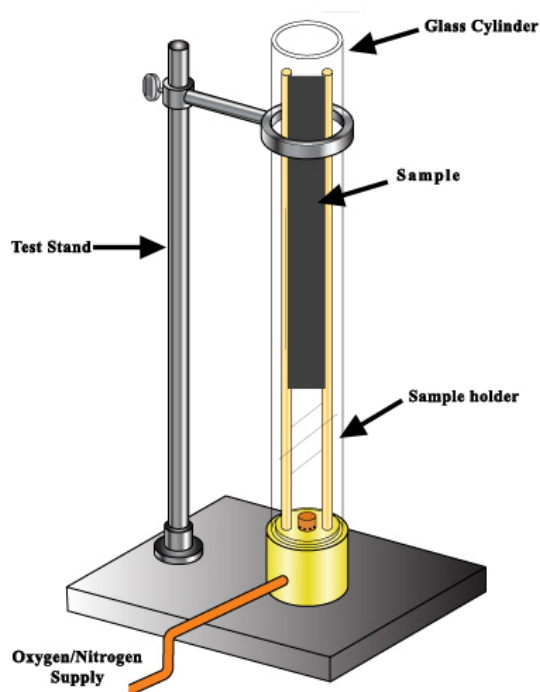


Figure 16. Typical LOI equipment.

The UL-94 test was previously performed on the materials obtained by the micro-extruder. In case of success, the UL-94 and LOI tests were carried out on the materials obtained by the larger scale extruder. All the reported results were obtained with materials prepared by the large extruder.

3.3.3. Fire behavior

Forced flame behavior was characterized by cone calorimeter (Fire Testing Technology, East Grinstead, UK) at an incident heat flux of 35 kW/m^2 according to **ISO 5660**. All samples ($100 \times 100 \times 3 \text{ mm}^3$) were wrapped in an aluminum foil and laid on a horizontal sample holder. With regard to the first set of materials, an additional edge frame was used to perform the tests. All measurements were repeated two or three times, so the results reported in the tables correspond to the mean values.

Cone calorimeter testing analyzes the behavior of products and materials when exposed to heat and a source of ignition. Due to the small size of specimens, cone calorimeter testing (Fig. 17) is a quick way to conduct research about fire performance of products whilst still in the development stage. This technique gets its name from the conical shaped heating element at which specimens are exposed. When exposed to the heat source, a spark ignites the sample leading to combustion. The cone calorimeter then gathers all the products of combustion in a duct, while oxygen and temperature measurements are used to calculate the energy that is produced. Testing can provide many parameters for each specimens, as

- the heat release rate (kW/m^2) throughout the duration of the test: the amount of energy given off by the specimen at any one time, for each meter squared area;
- the time to ignition of the specimen (s);
- the total heat release (MJ/m^2): the total energy given off per unit area of the sample;
- the smoke production (m^2) as well as the physical behavior, e.g. swelling or shrinking.

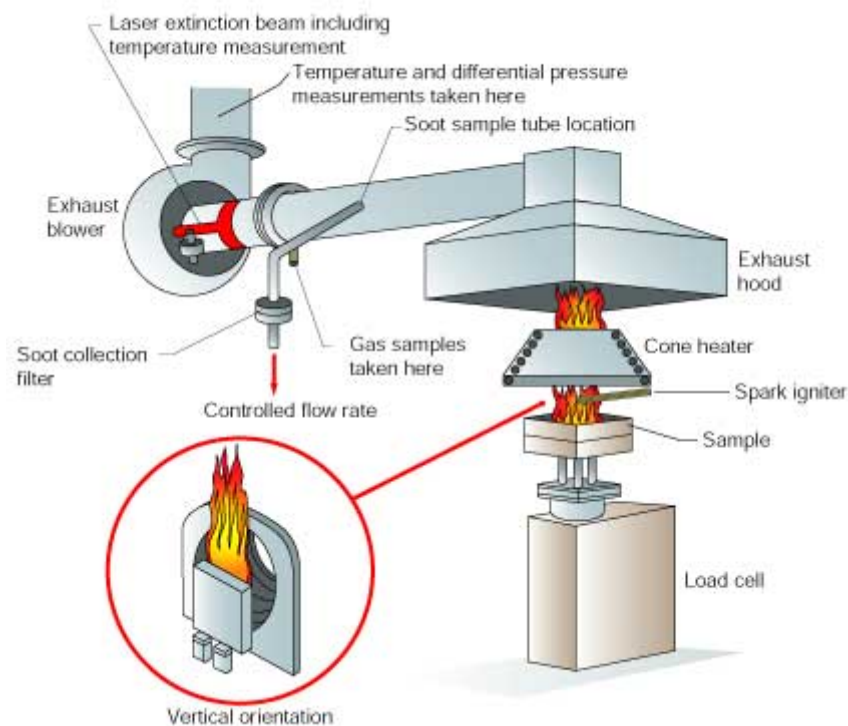


Figure 17. Cone calorimeter equipment.

Cone calorimeter provides a reliable means of measuring the rate of heat release, the single most important property predicting fire hazard, since it governs both the rate of fire growth and its maximum intensity. Tests are normally conducted with the sample in horizontal position, however it is possible to run tests in vertical orientation too.

3.3.4. Mechanical testing

The flexural strength and modulus were measured using a Tensometer 2020 testing machine (Alpha Technologies) according to **ISO 178**. The measurement was repeated five times for each type of material and the average value was calculated. The impact performances were obtained by using a pendulum Instron Ceast 9050, according to **ISO 179**. The specimens were tested using impact angle and energy respectively equal to 45° and 7.9 J. The reported values are the average ones.

3.3.5. Dynamic mechanical analysis (DMA)

Dynamic mechanical analysis is a widely used technique to characterize the properties of a material as a function of temperature, time and frequency. It works by applying a sinusoidal deformation to a sample of known geometry. The sample may be subjected to controlled stress or strain. In case of known deformation, the specimen requires a certain load, whose value is related to its stiffness. DMA measures stiffness and damping, respectively reported as modulus and $\tan\delta$. Due to the sinusoidal force, it is possible to express the modulus as two components, one in phase (storage modulus) and one out of phase (loss modulus). The storage modulus, either E' or G' , is the measure of the elastic behavior and it is numerically very similar to the Young modulus. The ratio of the loss modulus to the storage modulus is the $\tan\delta$ and is called damping because it represents the ability of the investigated materials to dampen mechanical loads. It is a measure of the energy dissipation of a material. DMA of the formulations was carried out by using a Tritec 2000 (Triton Technology) under the following conditions:

- strain 0.01 mm
- frequency 1 Hz
- temperature from -50 to 120°C
- nitrogen environment

3.3.6. Rheological analysis

Rheological tests at high shear rates provide important information about polymer processing (Fig. 18). Polymeric melts are non-Newtonian fluids and their viscosity decreases with increasing shear rate.

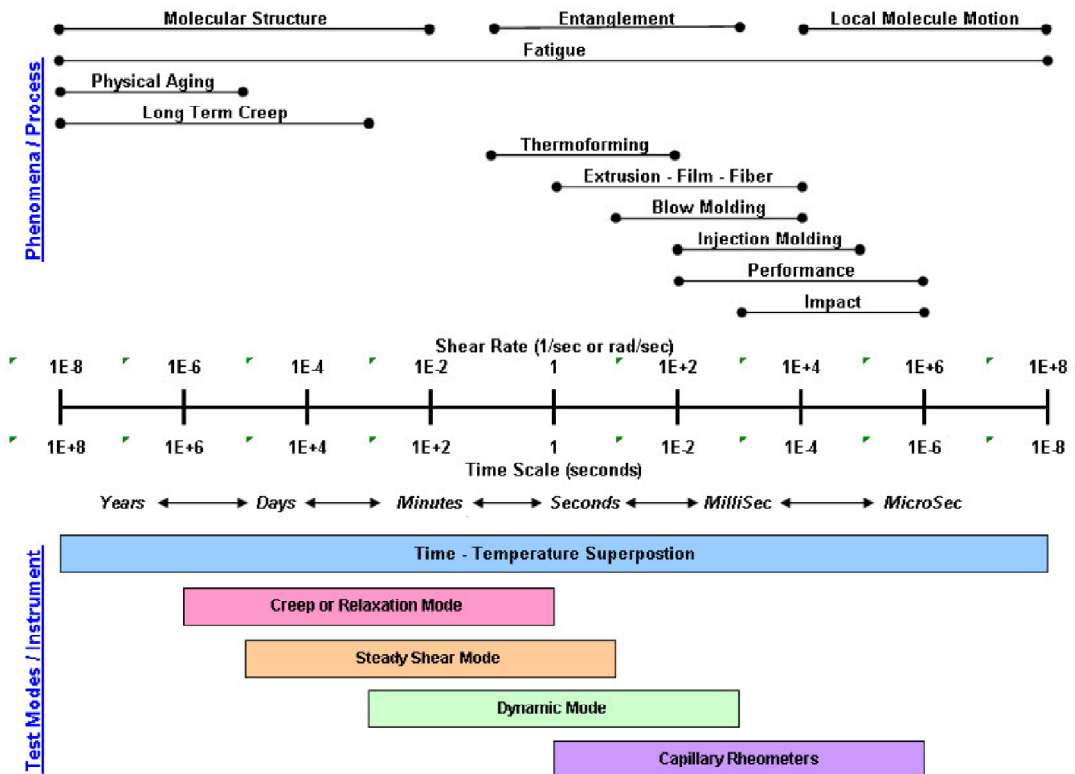


Figure 18. Importance of viscosity on processing conditions.

There are several parameters that can influence the viscosity properties. The molecular weight is the main structural parameter of melt flow behavior at temperatures above the T_g (for an amorphous material) or the melting point (for a semi-crystalline polymer). Melt viscosity is a constant at low shear rates. The viscosity in this region is known as the zero shear viscosity. For low molecular weight polymers, in which chain entanglement is not a factor, the zero shear viscosity is proportional to the molecular weight of polymers. Above a critical molecular weight, chains begin to entangle and the zero shear viscosity depends much stronger on molecular weight. Molecular weight distribution is also a fundamental parameter for the rheological properties. Beyond the Newtonian region, melt viscosity drops with increasing shear rate (shear thinning, Fig. 19). This behavior is the most important non-Newtonian property because it speeds up

material flow and reduces heat generation and energy consumption during processing. The size of shear thinning may be correlated with the molecular weight distribution: polymers with a broad distribution tend to become more thin at lower shear rates than those with a narrow distribution at the same average M_w . This has very important effects for industrial processes, e.g. molding and extrusion can be made easier by broadening the molecular weight distribution.

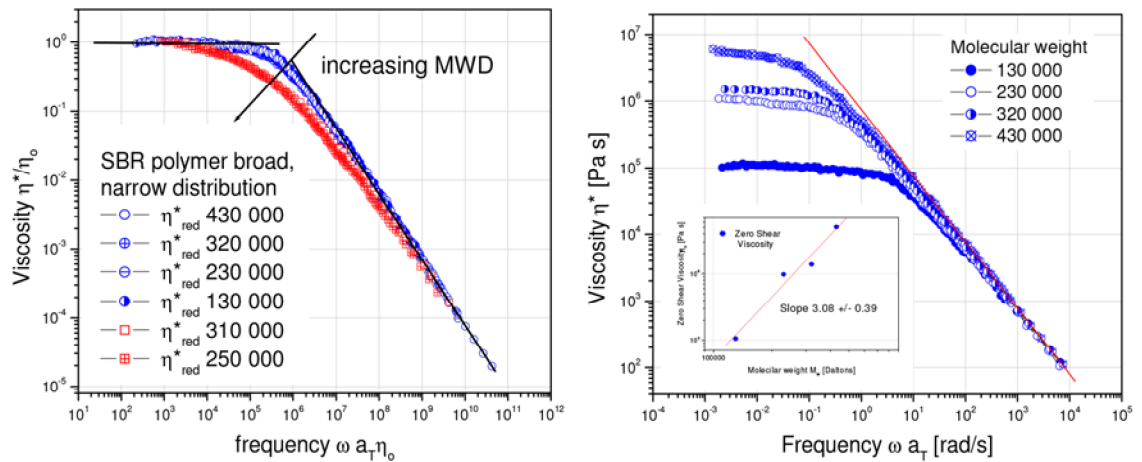


Figure 19. Relation between viscosity and molecular weight.

Branching and filler content should also be considered. Key factors are shape and size of fillers, as well as their concentration. Usually, adding fillers increases the melt viscosity, specially at low shear rates, and increase the non-Newtonian range. At higher shear rates the effect of the filler decreases and the matrix contributions dominate.

Processing conditions aside, rheological analysis at low shear rates may provide very useful information about the degree of dispersion of fillers inside polymers. Indeed rheological properties depend on the chemical structure, size, shape, surface modification of included particles but also on the interactions between fillers and matrix or the among the particles. The attractive forces among particles, especially in the case of nanoparticles, cause agglomeration with evident consequences for the viscosity. In the linear viscoelastic regime, G' gives an accurate indication of the nanoparticle dispersion: if a network is created, a plateau is visible in the terminal region (solid like behavior). Generally speaking, if the polymer is mainly viscous in nature, G'' is larger than G' but the addition of rigid particles may let G' become similar or even larger than G'' . Moreover every change in storage modulus is much more evident if compared to the loss modulus. Unfortunately, rheological tests alone can't determine the exact

morphology so often it is necessary to use complementary analysis such as electron or optical microscopy to assess the degree of dispersion.

Rheological behavior at high shear rates was investigated by using a capillary rheometer (Instron Ceast SR20) at 185°C. The diameter of the die was 1 mm and the shear rates values were 100, 200, 600, 1000, 2000, 6000 and 10000 s⁻¹. The second set of material underwent an additional analysis at low shear rates by using a TA Instrument AR-G2. Circular samples with a thickness of 1.0 mm were melted at 185 °C for 5 min in the parallel-plate fixture to eliminate the residual thermal history before measurements. To determine the linear region, dynamic strain sweep measurements were first conducted. Dynamic frequency sweep measurements were performed in the angular frequency (ω) range from 0.1 to 100 rad s⁻¹ at 185 °C.

3.3.7. Scanning electron microscopy (SEM)

SEM analysis was performed by using a Quanta FEI 200F instrument, whose accelerating voltage was 20 kV. The surface of all the samples, previously broken in liquid nitrogen, was sputter-coated with gold layer before examination. The second set of materials was studied using a Zeiss EVO MA10 instrument at the BAM in Berlin,. Both micrographs of broken samples and cone residues were taken.

3.3.8. Transmission electron microscopy (TEM)

TEM micrographs of the second set of materials were acquired by using a Tecnai G2 Instrument with an acceleration voltage of 120 kV. All the specimens were microtomed into 70 nm thick slices and deposited on a 400 mesh copper nets for observations.

CHAPTER 4: RESULTS AND DISCUSSION

4.1. Thermal stability

4.1.1. SEP and OSEP

TG and DTG data are summarized in Tab. 5 where T_{MAXn} represent the temperatures when maximum degradation rate occurs.

Pristine sepiolite underwent a multi-step dehydration process (Fig. 20) in accordance with the literature [64]. The mass loss was 15.6 wt% and it is mainly due to the water inside sepiolite. In particular, the DTG curves highlighted three different dehydration steps:

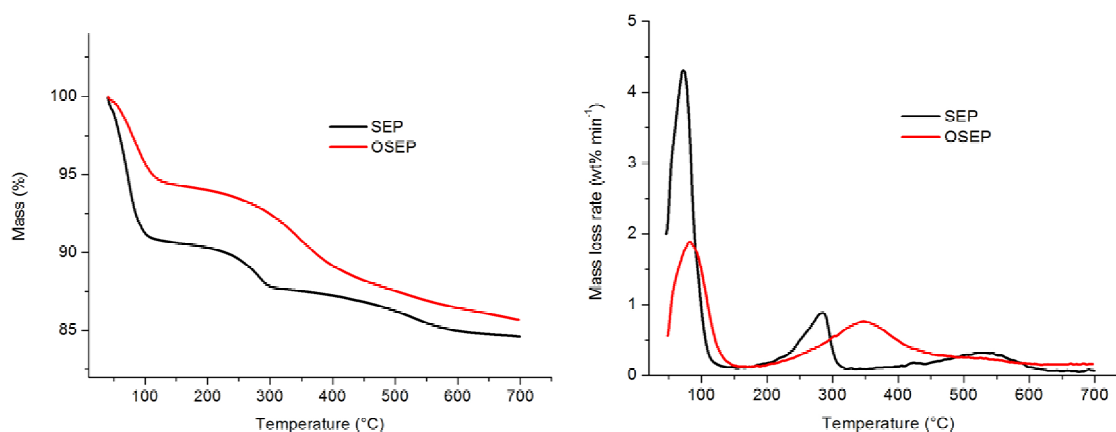
- first step (T_{MAX1} 71.6°C), due to the loss of zeolitic water and completed at 140.0°C
- second step (T_{MAX2} 284.5°C), it looked like a pretty broad peak and it was due to the coordinated water
- third step (T_{MAX3} 530.6°C), very broad peak due to the loss of coordinated water again

With regard to OSEP, the DTG curve showed a completely different behavior. The first peak was shifted from 71.6°C to 81.7°C and the mass loss rate was lower in comparison with SEP. There was only one more dehydration peak, whose maximum occurred at 348.9°C, due to the coordinated water. This result was in contrast to what expected: in the case of organically modified sepiolite, two peaks should have appeared in the range 200-700°C [64] because the thermal decomposition involves both physically and chemically bonded modifier. This suggested that the surfactant was bonded to the sepiolite in only one way, either physically or chemically. This outcome was surely due to the peculiar reaction conditions used to prepare OSEP.

Table 5.

Thermogravimetric outcomes of SEP and OSEP.

	40-140°C		140-330°C		330-650°C	
	Mass loss (%)	T _{MAX1} (°C)	Mass loss (%)	T _{MAX2} (°C)	Mass loss (%)	T _{MAX3} (°C)
SEP	9.4 ± 0.3	71.6 ± 1	3.0 ± 0.1	284.5 ± 2	2.9 ± 0.1	530.6 ± 2
OSEP	5.4 ± 0.2	81.7 ± 1	3.1 ± 0.1	348.9 ± 3	5.5 ± 0.2	-

**Figure 20.** Thermal stability of SEP and OSEP.

4.1.2. First set of materials

TG and DTG curves of the first set of materials are showed in Fig. 21. T_{5%}, T_{MAX} and M_{MAX} are respectively the temperatures at 5% mass loss, the maximum degradation rate temperature and the maximum mass loss rate.

The thermal decomposition of PP, in nitrogen, started at 313°C. At 460°C the polymer was completely consumed and no residue remained. The decomposition took place in a single step and the DTG maximum occurred at 433.2°C. Addition of 1 wt% pristine sepiolite increased the thermal stability and decomposition temperature of PP, as pointed out by the T_{5%} and T_{MAX} values. The M_{MAX} was instead the same if compared to PP. Similarly to the resin, there was a single decomposition step but characterized by a DTG maximum at 476.9°C, leaving a negligible amount of residue at 700°C.

As reported in Tab. 6, adding the flame retardant did not significantly change the T_{5%} value but the decomposition rate was much lower in comparison with PP, owing to the effectiveness of the flame retardant. There was an interesting outcome: both the EX based formulations had the same thermal stability, even if the amount of EX was different (25 or 18 wt%). The TG curve showed that the thermal stability of

PP/18EX/1SEP was a little lower than that of PP/18EX. This was unexpected, having considered the big increase of stability observed for PP/1SEP. The DTG curve showed that the decomposition temperature is higher than that of PP and, above all, the mass loss rate was much lower in comparison to all the other formulations, suggesting a synergistic effect between SEP and EX as will be shown later. This synergistic effect also influenced the residue amount, which resulted to be higher than those of PP/18EX and PP/25EX.

Table 6.

TGA results of the first set of materials.

Sample	T _{5%} (°C)	T _{MAX} (°C)	M _{MAX} (wt% min ⁻¹)	Residue 700°C (wt%)
PP	360.2 ± 5	433.2 ± 2	50.9 ± 1	-
PP/1SEP	423.7 ± 4	476.9 ± 2	50.9 ± 1	1.3 ± 0.1
PP/18EX	372.5 ± 4	479.6 ± 2	39.1 ± 2	8.9 ± 0.3
PP/18EX/1SEP	359.6 ± 3	477.8 ± 2	29.8 ± 2	11.3 ± 0.7
PP/25EX	371.2 ± 4	478.3 ± 3	41.1 ± 1	10.2 ± 0.5

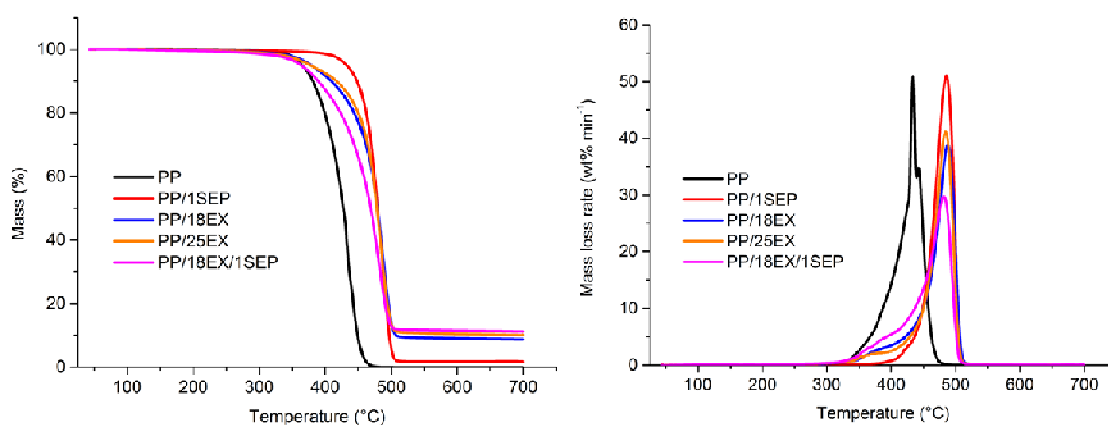


Figure 21. TGA of the first set of composites (nitrogen flux).

4.1.3. Second set of materials

TG and DTG curves are showed in Fig. 22 and Fig. 23, while the data are reported in Tab. 7 and Tab. 8. Again, T_{5%}, T_{MAXn} and M_{MAX} represent the temperatures at 5% mass loss, the temperatures when maximum mass loss rate occurs and the maximum mass loss rate, respectively.

As showed in Fig. 22, all the formulations decomposed in nitrogen through one single step with a residue at 700 °C almost nil in the case of PP, PP/0.5SEP, PP/0.5OSEP, but equal approximately to 4.3 and 6.3 wt% in presence of 12% and 15 wt% Exolit AP766. The partial decomposition of these residues at higher temperatures allowed to assume a carbonaceous-inorganic nature of them. Adding 0.5 wt% SEP didn't significantly affect the $T_{5\%}$ of the matrix, whereas a small increase of the same thermal parameter was detected for PP/0.5OSEP. On the contrary, the modification of the matrix by inclusion of the flame retardant worsened its thermal stability with an effect increasing with the ET content. Furthermore, this effect was not recovered by the simultaneous inclusion of sepiolite nanoparticles, pristine or organically modified. Although the thermal decomposition of investigated materials is mainly controlled by the degradation pathway of the resin, the above mentioned effects may be attributed to slight filler-matrix interactions affecting the decomposition mechanisms as also witnessed, in all cases, by the increase of the T_{MAX} value, almost equal to 10°C in all cases, and by the reduction of the M_{MAX} values. These results demonstrate that both SEP and OSEP did not significantly influence the decomposition characteristics controlled by the intumescent additive.

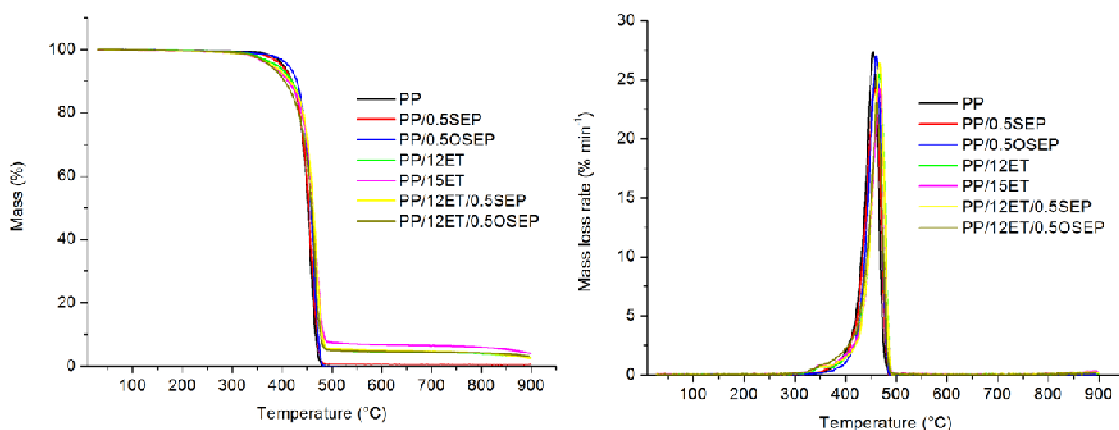


Figure 22. TGA of the second set of composites (nitrogen flux).

Table 7.

Thermal stability of the second set of materials (nitrogen flux).

Sample	T _{5%} (°C)	T _{MAX} (°C)	M _{MAX} (wt% min ⁻¹)	Residue 700°C (wt%)	Residue 900°C (wt%)
PP	400.2 ± 7	456.7 ± 1	28.6 ± 1.5	-	-
PP/0.5SEP	401.6 ± 4	464.7 ± 2	25.3 ± 0.5	0.5 ± 0.2	0.5 ± 0.2
PP/0.5OSEP	410.5 ± 5	465.0 ± 2	27.8 ± 1	0.1 ± 0.1	0.1 ± 0.1
PP/12ET	387.3 ± 7	468.5 ± 1	25.6 ± 1	4.3 ± 0.5	3.5 ± 0.5
PP/15ET	377.7 ± 4	467.8 ± 1	24.2 ± 0.5	6.3 ± 0.5	4.3 ± 0.5
PP/12ET/0.5SEP	380.7 ± 4	468.3 ± 1	26.7 ± 0.5	4.6 ± 0.1	2.6 ± 0.1
PP/12ET/0.5OSEP	379.0 ± 7	469.0 ± 3	24.3 ± 1.5	4.4 ± 0.5	3.4 ± 0.5

In Fig. 23, the mass loss (TG) and the derivative mass loss (DTG) curves of all studied materials, obtained by heating samples in air, are presented. In this case, PP decomposed in two steps: the main one represented by a high and sharp signal at 314.4°C and the second one by an asymmetric and much less pronounced signal at about 500°C. This behavior is attributed to a radical chain process which leads to the release of volatile molecules such as alcohols, aldehydes and ketones. Moreover, thermo-oxidative decomposition of PP led to a carbonaceous char residue, which resulted to be always almost completely degraded for further heating up to 900 °C.

From parameters collected in Table 8, it is evident that the inclusion of SEP or OSEP particles slightly affected the thermal degradation mechanisms of the matrix reducing only the height of the first derivative signal.

The intumescent flame retardant, instead, increased the thermal stability and changed the decomposition pathway: an additional differential signal, due to the decomposition of ammonium polyphosphate to yield polyphosphoric acid, ammonia and water is revealed. This signal, centered at about 280°C for the system containing 12 wt% of ET, is shifted to lower temperature by increasing the fire retardant content and for formulations involving SEP/OSEP particles simultaneously. For these systems, the main DTG signal is shifted to higher temperatures with respect to the formulations without the flame retardant and it is further reduced in height. At the same time, the peak temperature of the third derivative signal is also increased even if to a less extent than the main one.

Regarding the residue, it amounted at about 25 wt% after the main decomposition step, five times higher than PP. The carbonaceous-inorganic residue decomposed in a subsequent third step, when the materials were heated up to 900°C, led residues between 3.4 to 5.5 wt% quite similar to the final residues observed for the thermal decomposition. Similar decomposition characteristics observed in presence of sepiolite allowed to assume that these latter did not improve the thermo-oxidative stability of the char.

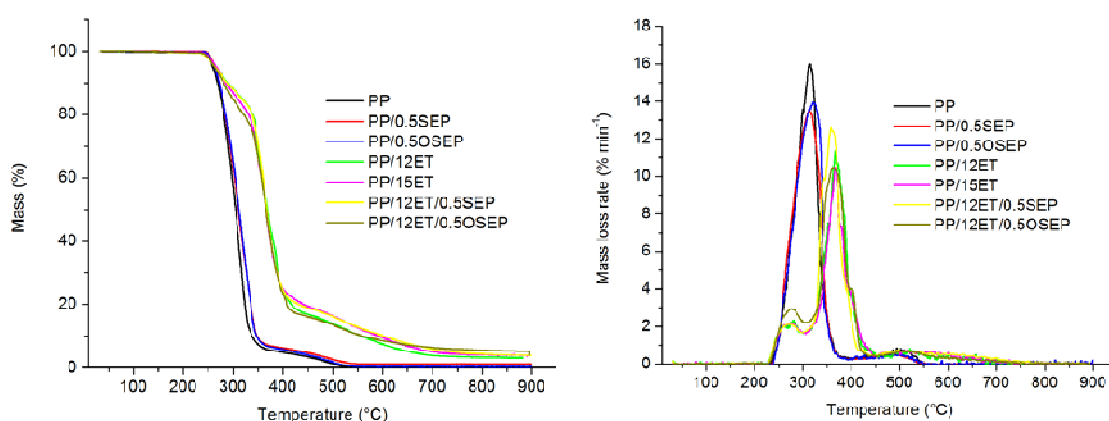


Figure 23. TGA of the second set of materials (synthetic air).

Table 8.

Thermal stability of the second set of materials (synthetic air flux).

Sample	T _{5%} (°C)	T _{MAX1} (°C)	T _{MAX2} (°C)	Residue 405°C (wt%)	T _{MAX3} (°C)	M _{MAX} (wt% min ⁻¹)	Residue 900°C (wt%)
PP	259.8 ± 4	-	314.4 ± 3	4.8 ± 0.1	502.9 ± 6	16.0 ± 0.7	-
PP/0.5SEP	264.4 ± 1	-	313.3 ± 5	6.1 ± 0.1	479.9 ± 3	13.9 ± 1.5	1.0 ± 0.1
PP/0.5OSEP	262.7 ± 4	-	321.9 ± 5	5.7 ± 0.3	492.2 ± 3	13.9 ± 0.7	0.3 ± 0.2
PP/12ET	265.5 ± 1	280.4 ± 2	366.4 ± 2	24.6 ± 1.1	521.9 ± 1	11.5 ± 0.6	3.4 ± 0.3
PP/15ET	267.3 ± 1	275.1 ± 1	367.4 ± 2	29.9 ± 1.5	514.4 ± 1	10.4 ± 0.2	4.2 ± 0.2
PP/12ET/0.5SEP	264.4 ± 1	271.1 ± 2	358.1 ± 2	24.6 ± 0.3	497.9 ± 2	12.7 ± 0.6	4.4 ± 0.1
PP/12ET/0.5OSEP	263.3 ± 1	273.9 ± 2	366.1 ± 3	23.4 ± 1.3	515.4 ± 3	10.9 ± 0.2	5.5 ± 1.0

4.2. DSC analysis

4.2.1. First set of materials

The DSC analysis of PP showed that the degree of crystallinity was about 36% (Tab. 9). The addition of 1 wt% pristine sepiolite slightly shifted both the melting and crystallization temperatures. Moreover the heat of crystallization increased by 6.7%, indicating the nucleating effect of the filler. Adding 18 wt% of flame retardant did not modify either the melting temperature of PP or the degree of crystallinity. The interesting outcome was the lower crystallization temperature (-7.7°C) in comparison with PP, probably due to impediments to the matrix crystallization in presence of the intumescent additive. The same effect was observed for PP/18EX/1SEP but, in this case, it was slightly less evident. On the other hand, no significant change of degree of crystallinity was noticed.

Table 9.

DSC results of the first set of materials.

	T_m ($^{\circ}\text{C}$)	ΔH_m (J/g)	T_c ($^{\circ}\text{C}$)	ΔH_c (J/g)	χ_c (%)
PP	167.2 ± 0.2	74.9 ± 3	127.5 ± 0.3	75.5 ± 3	36 ± 1
PP/1SEP	166.0 ± 0.2	73.2 ± 2	126.5 ± 0.3	80.5 ± 2	36 ± 1
PP/18EX	167.6 ± 0.5	66.7 ± 4	121.5 ± 0.2	70.0 ± 3	37 ± 2
PP/18EX/1SEP	167.4 ± 0.5	62.2 ± 2	123.8 ± 0.3	63.8 ± 1	37 ± 1
PP/25EX	167.2 ± 0.4	63.7 ± 2	119.5 ± 0.3	68.5 ± 1	36 ± 1

4.2.2. Second set of materials

Just as observed for PP/1SEP, the addition of a very small amount of SEP (0.5 wt%) didn't change the properties of the matrix considerably: the increase of the degree of crystallinity was negligible if the uncertainty was taken into account (Tab. 10). The presence of OSEP didn't affect the crystallinity but it resulted in a small decrease of the crystallization temperature. This outcome, absent in the SEP based formulation, was likely due to the organic surfactant inside the filler. The presence of 12 wt% ET caused a small decrease of the melting and crystallization temperatures in comparison with PP. Just as happened with EX, the degree of crystallinity was not affected by the presence of the flame retardant. The addition of 15 wt% ET led to the same result. The simultaneous

presence of flame retardant and SEP didn't affect the properties of the matrix, on the other hand a completely different result was observed for the formulation containing ET and OSEP: a significant increase of the degree of crystallinity occurred, clue of a better conformation of the macromolecules.

Table 10.
DSC results of the second set of materials.

	T_m (°C)	ΔH_m (J/g)	T_c (°C)	ΔH_c (J/g)	χ_c (%)
PP	167.2 ± 0.2	74.9 ± 3	127.5 ± 0.3	75.5 ± 3	36 ± 1
PP/0.5SEP	167.9 ± 0.2	76.5 ± 3	127.4 ± 0.2	77.8 ± 3	37 ± 1
PP/0.5OSEP	168.5 ± 0.1	75.7 ± 1	126.2 ± 0.2	78.6 ± 1	36 ± 1
PP/12ET	166.0 ± 0.2	69.5 ± 3	125.2 ± 0.4	73.5 ± 3	36 ± 2
PP/15ET	166.3 ± 0.2	69.7 ± 3	125.9 ± 0.4	70.5 ± 3	37 ± 2
PP/12ET/0.5SEP	166.1 ± 0.1	68.6 ± 3	126.0 ± 0.3	71.4 ± 3	38 ± 1
PP/12ET/0.5OSEP	166.3 ± 0.2	73.4 ± 1	126.9 ± 0.1	75.0 ± 1	41 ± 1

4.3. Flammability and ignitability

4.3.1. First set of materials

PP was a highly combustible material as confirmed by the LOI value (20.8 vol%) and the failure in UL-94 test (Tab. 11). The addition of 1 wt% sepiolite resulted in a worsening in LOI so even such small amount of filler was enough to deteriorate the flammability of the matrix. This outcome was in contrast with the TG results, which showed a retarded decomposition as pointed out by the $T_{5\%}$ and T_{MAX} values. The UL-94 failed as well, indeed the specimen burned completely. The presence of the flame retardant in PP/18EX did affect the LOI, increased from 20.8 to 25.2 vol%. This percentage allowed to lower the flammability but not enough to achieve the V-0 level. Several tests showed that the minimum amount to obtain the V-0 level was equal to 25 wt%, this also permitted to increase the LOI up to 30.9 vol% (+48% compared to the pristine matrix). The oxygen index of the EX/SEP based formulation was equal to 26.5%, a value slightly higher than the one obtained by PP/18EX. The combination of both additives improved the flammability behavior and resulted in a V-0 ranking: this was a clear indication of a synergistic effect between sepiolite and the flame retardant.

The following equation was used to quantify the synergism between SEP and EX with regard to the LOI performance:

$$SE = (OI_{FR+S+P} - OI_P) / ((OI_{FR+P} - OI_P) + (OI_{S+P} - OI_P))$$

where OI_{FR+S+P} is the oxygen index of the polymer filled with flame retardant and synergist, OI_{FR+P} is the oxygen index of the polymer filled with flame retardant, OI_{S+P} is the oxygen index when only the synergist is included and OI_P is the oxygen index of the pristine polymer [68]. In this case, the obtained value was equal to 1.5, not very high because of the negative effect of the sepiolite on the flammability properties. The synergism was also measured assuming a superposition of the effect of the single additives (Tab. 11).

Table 11.
Flammability properties of the first set of materials.

Sample	LOI (vol%)	Cal. LOI for superposition (vol%)	UL-94	Flaming dripping
PP	20.8 ± 0.2	-	-	Yes
PP/1SEP	20.1 ± 0.2	-	-	Yes
PP/18EX	25.2 ± 0.2	-	V-2	Yes
PP/18EX/1SEP	26.5 ± 0.2	24.5	V-0	No
PP/25EX	30.9 ± 0.2	-	V-0	No

4.3.2. Second set of materials

The UL-94 and LOI results of the formulations are summarized in Tab. 12. Adding 0.5 wt% SEP decreased the LOI of the matrix but the effect was quite negligible. The worsening was more apparent when OSEP was added to the resin. This decrease in LOI was not explained by an earlier decomposition, as witnessed by the increased $T_{5\%}$ and T_{MAX} values, but considering a reduced melt flow. The bad performances of PP, PP/0.5SEP, and PP/0.5OSEP were also confirmed by their failure in the UL-94 test. The minimum amount of ET necessary to achieve the V-0 classification was equal to 15 wt%, this percentage also allowed to increase the LOI from 20.8 to 25.4 vol%. The same LOI was achieved by PP/12ET/0.5SEP, which

therefore showed a higher LOI than PP/12ET. Nevertheless this material didn't succeed in the UL-94 test and burned completely with dripping phenomena. The most interesting outcome was obtained by PP/12ET/0.5OSEP, which outperformed the ET/SEP based formulation in LOI and UL-94. Indeed it achieved the V-0 ranking and the highest LOI of all the investigated materials. PP/12ET/0.5OSEP showed also a higher LOI than PP/15ET despite the lower amount of flame retardant.

The performance of PP/12ET/0.5OSEP was surely due to a synergistic effect between ET and OSEP, since adding OSEP alone only deteriorated the LOI. Applying the below formula wasn't appropriate because dividing by a negative value delivered uncertain results. The origin of the synergy between ET and OSEP was likely due to an additional mechanism or phenomenon occurring only in this combination.

$$SE = (OI_{FR+S+P} - OI_P) / ((OI_{FR+P} - OI_P) + (OI_{S+P} - OI_P))$$

Table 12.
Flammability results of the second set of materials.

Sample	LOI (vol%)	Cal. LOI for superposition (vol%)	UL-94	Flaming dripping
PP	20.8 ± 0.2	-	-	Yes
PP/0.5SEP	20.0 ± 0.2	-	-	Yes
PP/0.5OSEP	19.2 ± 0.2	-	-	Yes
PP/12ET	22.3 ± 0.2	-	V-2	Yes
PP/15ET	25.4 ± 0.2	-	V-0	No
PP/12ET/0.5SEP	25.7 ± 0.3	21.5	V-2	Yes
PP/12ET/0.5OSEP	26.3 ± 0.4	20.7	V-0	No

4.4. Fire behavior

The fire behavior was investigated using a Fire Testing Technology cone calorimeter with a heat flux of 35 kW/m², which is the recommended heat flux for exploratory testing.

The heat release rate (HRR), total heat released (THR) and total heat evolved (THE) were discussed. THR is the integral of HRR with respect to time and THE is the THR at the end of the test. THE and HRR are mathematically related, but represent independent

fire hazards: THE depends strongly on the total mass loss, the effective heat of combustion of the volatiles and the combustion efficiency in the flame zone. Smoke production rate (SPR) and total smoke release (TSR), resulting from incomplete combustion, were evaluated to determine the fire hazard. PHRR value is strongly dependent on the fire scenario as well as the intrinsic fire properties of the specimen and represents the most used result from cone calorimeter.

There are two indices that allow to simplify the interpretation of cone calorimeter data, FIGRA and MARHE. The first one (fire growth rate index) is the maximum quotient of $HRR(t)/(t)$ and usually it is calculated by dividing the peak heat release rate by time to peak heat release rate. It is a very useful index since it can estimate both the fire spread rate and the size of a fire. The second index (maximum average rate of heat emission) is defined as the cumulative heat emission divided by time and its peak value and can be considered a good measure of the tendency for fire development under real conditions. These indices allow to assess the hazard of developing fires so they are useful to get immediately a qualitative estimate of flame retardancy.

4.4.1. First set of materials

As expected, PP was really easy to burn: the HRR curve was characterized by a sharp peak whose maximum was at 610 kW/m^2 (Fig. 24). This high value resulted in large values for all the indices, such as THE, FIGRA and MARHE.

Addition of SEP didn't change the fire properties of the matrix dramatically: the PHRR value was a bit lower than that of PP, the shape of the HRR, THR and TSP curves was substantially identical if compared to the resin. The FIGRA and MAHRE indices were practically unchanged as well (Tab. 13). Sepiolite made the ignition harder to occur, this was in agreement with the retarded thermal decomposition of PP/1SEP observed in TG analysis. Adding 18 wt% EX wasn't enough to obtain the V-0 level, nevertheless it could clearly improve the fire behavior, indeed the PHRR and THE values decreased by 81% and 46% respectively. The HRR curve didn't show any sharp peak but, rather, an irregular trend with two maxima at 55 and 175 s (Fig. 25). MARHE and FIGRA indices showed a significant reduction if compared to PP, as evidence of the effectiveness of the flame retardant. Increasing the EX amount from 18 to 25 wt% (minimum percentage necessary to pass the UL-94 test) obviously improved the fire performance.

Table 13.
Results of the cone calorimeter measurements.

	TTI (s)	PHRR (kW/m ²)	THE (MJ/m ²)	FIGRA (kW/m ² s)	MARHE (kW/m ²)	CO yield (kg/kg)
PP	47 ± 3	610 ± 45	72 ± 5	4.1 ± 0.4	255 ± 6	0.035 ± 0.002
PP/1SEP	56 ± 3	547 ± 40	67 ± 5	3.8 ± 0.2	223 ± 9	0.057 ± 0.003
PP/18EX	27 ± 4	115 ± 14	39 ± 2	2.1 ± 0.4	91 ± 2	0.034 ± 0.002
PP/25EX	30 ± 3	72 ± 3	15 ± 2	2.4 ± 0.1	38 ± 2	0.044 ± 0.003
PP/18EX/1SEP	29 ± 2	102 ± 4	18 ± 3	2.0 ± 0.1	53 ± 2	0.023 ± 0.002

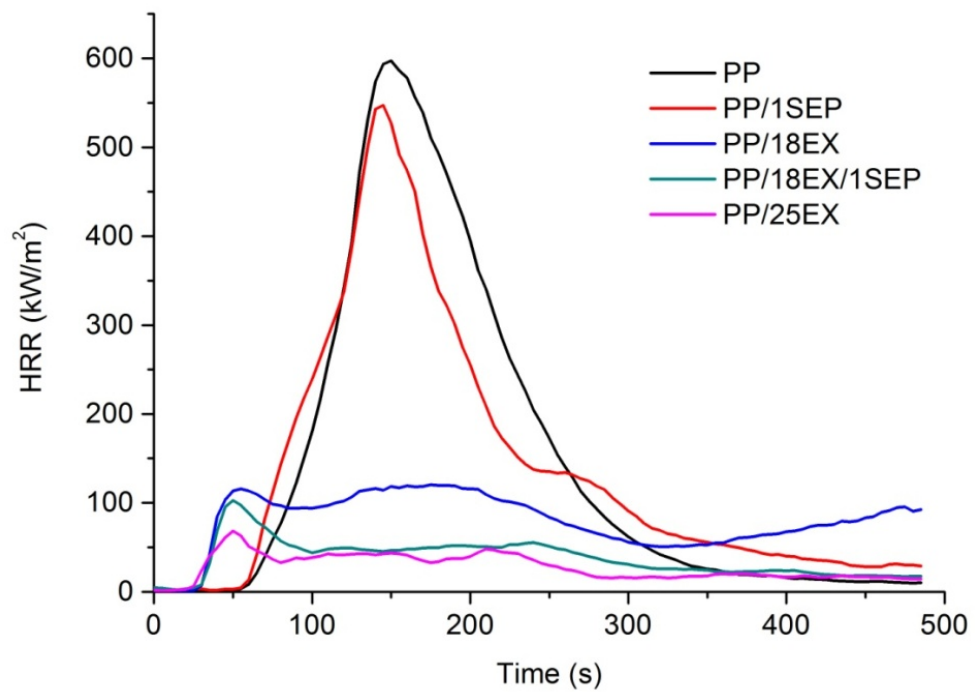


Figure 24. HRR curve of the first set of formulations.

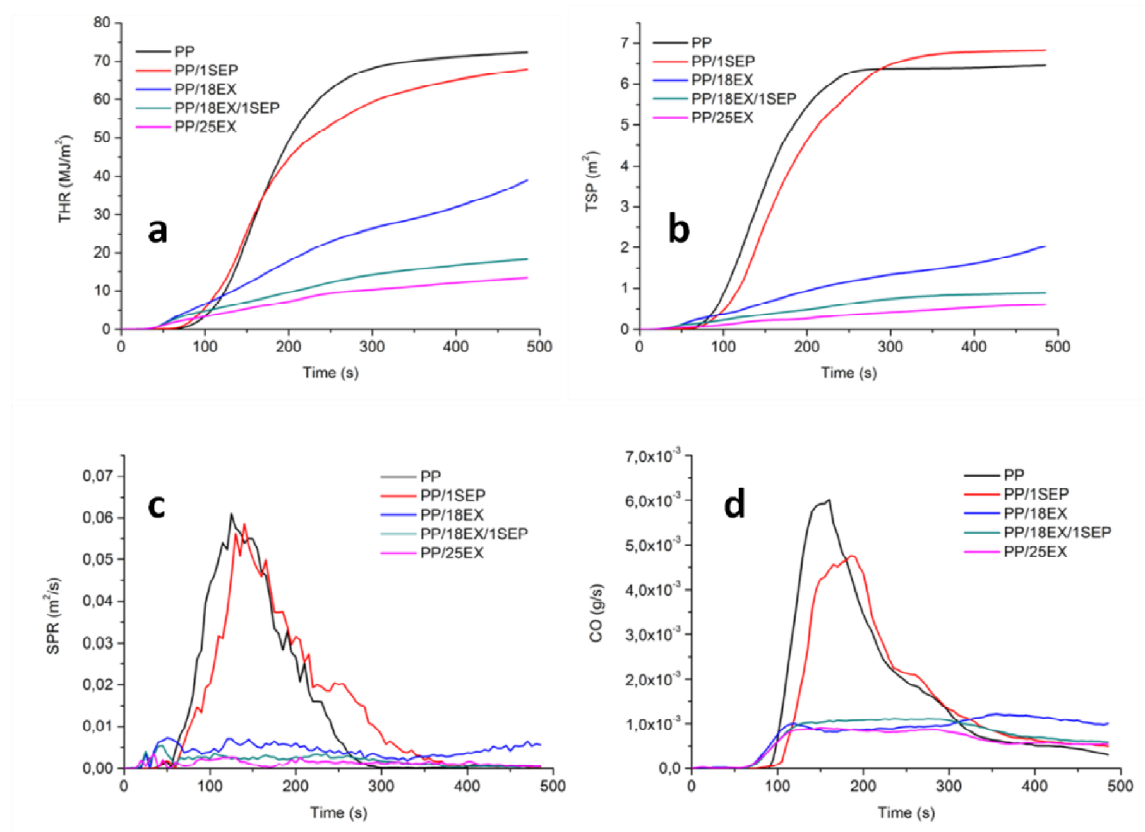


Figure 25. THR (a), TSP (b), SPR (c) and CO production (d).

4.4.2. Second set of materials

Figure 26 shows the HRR and the THR curves of the investigated materials while Table 14 summarizes key parameters reflecting their fire performance like TTI, PHRR, total heat evolved (THE = THR at end of test), FIGRA and MARHE. Table 15 instead shows the modes of action of the included flame retardants: the residue percentages, the THE/TML ratios, the reduction (Δ) in THE and PHRR. Using these parameters the reduction due to charring and flame inhibition (Cal. $\Delta\text{FR}_{(\text{CF})}$) was calculated, as well as the reduction in PHRR caused by an additional protective layer effect (Cal. $\Delta\text{FR}_{(\text{PROT. LAYER})}$).

As expected, PP was very easy to burn: its HRR curve showed a sharp peak at a very high PHRR (1610 kW/m^2) and the duration of burning was only 200 s (Fig. 26). The high PHRR also resulted in high values for all the indices, FIGRA, MARHE and PHRR/t(PHRR). The high THR indicated a high fire load, the violent burning of PP was caused by its high effective heat of combustion, witnessed by the ratio of THE/TML and the lack of residue (Table 15). The addition of 0.5 wt% SEP or OSEP influenced neither the fire behavior of PP and the amount of residue nor the effective heat of

combustion. On the other hand, these fillers favored ignition, as demonstrated by the shorter TTI values in comparison with PP. However, considering that the thermogravimetric analysis did not highlight any influence on thermal and thermo-oxidative decomposition, the worsening in TTI was attributed to a more quick increase of the surface temperature.

The binary systems PP/12ET and PP/15ET showed a clear reduction of the PHRR value, respectively equal to 68% and 79% if compared to PP. These formulations also manifested a marked drop in the PHRR, FIGRA, MARHE and PHRR/t(PHRR) parameters, moreover the HRR curves were broad with several maxima. In contrast to PP, these systems burned as residue-forming materials showing a reduction in the THE equal to 8% and 16% in presence of 12 wt% and 15 wt% ET, respectively. The reduction in fire load (THE) was caused by the limited amount of residue and a significant drop in THE/TML. The contribution of the different modes of action is quantified in Table 15. With respect to HRR, the main mode of action was the protective intumescent layer, the THE was instead controlled by the charring and the reduction in the effective heat of combustion of the volatiles (THE/TML).

With respect to PHRR, the protective layer effect became the most pronounced mode of action, with reduction between 65 and 85%. The HRR curve of PP/12ET/0.5SEP nearly resembled that of PP/15ET, despite the lower amount of flame retardant. The simultaneous presence of ET and OSEP in PP/ET/OSEP allowed the largest reduction in PHRR, accompanied by the longest burning time. Comparing the reduction due to the protective effect of PP/12ET/0.5SEP and PP/12ET/0.5OSEP with PP/12ET identified the remarkably improved residual protective layer as the origin of synergistic behavior. The protective layer effect was so strong that the contribution of the charring and the reduction in THE/TML became quite negligible.

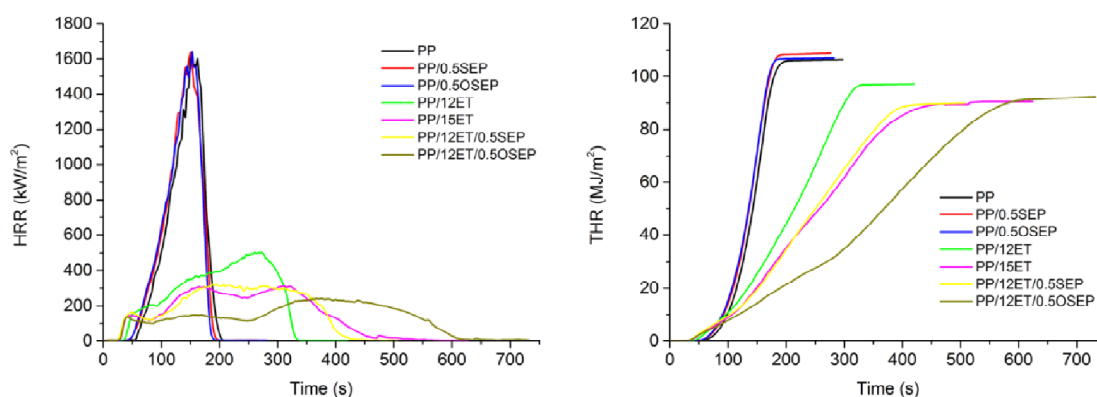


Figure 26. HRR and THR curves of the second set of materials.

Table 14.
Result of the cone calorimeter tests: performance

	TTI (s)	PHRR (kW/m ²)	THE (MJ/m ²)	FIGRA (kW/sm ²)	MAHRE (kW/m ²)	PHRR/t(PHRR) (kW/s m ²)	CO yield (kg/kg)
PP	54 ± 3	1610 ± 70	106 ± 4	10.7 ± 1	573 ± 20	10.7	0.032 ± 0.003
PP/0.5SEP	48 ± 2	1701 ± 70	108 ± 1	11.7 ± 0.2	580 ± 9	11.7	0.033 ± 0.001
PP/0.5OSEP	46 ± 4	1665 ± 40	106 ± 1	10.6 ± 0.4	592 ± 2	10.7	0.035 ± 0.001
PP/12ET	37 ± 1	510 ± 36	97 ± 3	2.4 ± 0.1	301 ± 5	2.0	0.077 ± 0.005
PP/15ET	27 ± 1	339 ± 30	89 ± 1	3.4 ± 0.1	226 ± 20	1.0	0.063 ± 0.004
PP/12ET/0.5SEP	27 ± 2	320 ± 30	88 ± 1	3.3 ± 0.3	227 ± 2	1.7	0.050 ± 0.006
PP/12ET/0.5OSEP	28 ± 1	241 ± 3	92 ± 2	3.1 ± 0.1	159 ± 5	0.6	0.041 ± 0.003

Table 15.
Modes of action of the flame retardants

	Residue (wt%)	THE/TML (kW/g m ²)	Weight (g)	Cal. ΔFR _(CF) (%)	ΔTHE (%)	ΔPHRR (%)	Cal. ΔFR (PROT. LAYER) (%)
PP	-	4.3 ± 0.2	23.5				
PP/0.5SEP	-	4.5 ± 0.05	23.9	-6.4	-1.8	-5.7	-
PP/0.5OSEP	-	4.4 ± 0.05	23.7	-3.2	0.0	-3.4	-
PP/12ET	6.5 ± 0.3	3.8 ± 0.05	26.0	8.6	8.5	68.3	65.4
PP/15ET	6.0 ± 0.4	3.9 ± 0.03	25.0	9.3	16.0	78.9	75.8
PP/12ET/0.5SEP	6.9 ± 0.7	3.7 ± 0.05	25.7	12.4	17.0	80.1	76.6
PP/12ET/0.5OSEP	5.6 ± 0.1	3.9 ± 0.1	25.1	8.6	13.2	85.0	83.2

As displayed in Fig. 27, the smoke production of PP, PP/0.5SEP and PP/0.5OSEP were pretty identical. The addition of 12 wt% of flame retardant made the smoke production twice larger. PP/15ET, PP/12ET/0.5OSEP, and PP/12ET/0.5OSEP showed an increase in smoke production as well, even though less pronounced than PP/12ET. Comparing the smoke production rates with the HRR curves proved that the smoke yield was strongly increased. This outcome was consistent with the increase in CO yield (Tab. 14). Two reasons were proposed to explain this behavior: an incomplete combustion, in accordance with the large reduction in THE/TML, and the decomposition of the intermediate stable char.

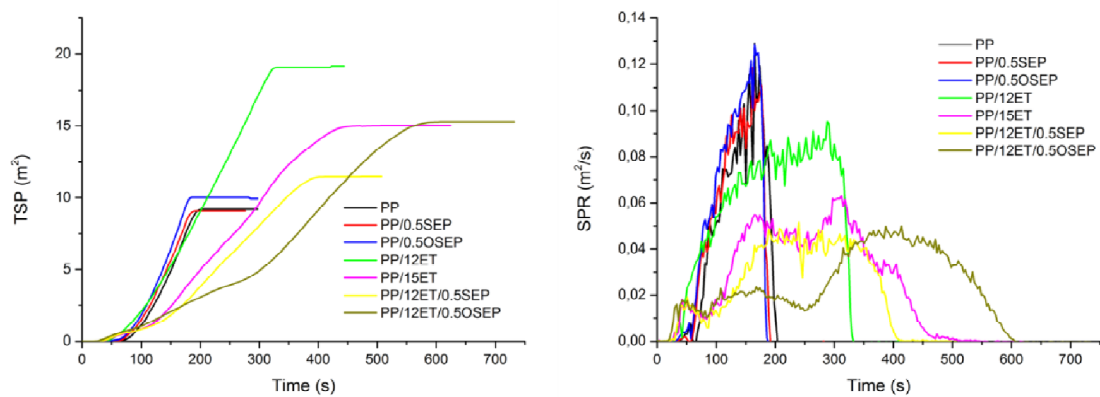


Figure 27. TSP and SPR curves of the second set of materials.

4.5. Mechanical properties

4.5.1. First set of materials

Adding SEP didn't change either the flexural modulus or strength of PP, as showed in Tab. 16. Including 18 wt% EX instead had a negative effect on the mechanical properties, indeed the modulus decreased by 5%, on the contrary no effect was observed for the flexural strength. Adding a higher percentage of the flame retardant worsened the modulus even more but, again, the flexural strength was unaffected. The unexpected outcome was obtained with PP/18EX/1SEP (Fig. 28) showing a pretty large increase of the modulus (+13% and +20% if compared to PP and PP/18EX).

Table 16.
Mechanical properties of the first set of materials.

	Flexural modulus (MPa)	Flexural strength (MPa)	Modulus variation (%)	Strength variation (%)
PP	1402 ± 25	33.2 ± 0.6	-	-
PP/1SEP	1400 ± 29	33.4 ± 0.5	-0.1	0.6
PP/18EX	1334 ± 30	33.2 ± 0.4	-4.7	-
PP/25EX	1310 ± 25	33.1 ± 0.4	-6.4	-0.3
PP/18EX/1SEP	1588 ± 26	33.1 ± 0.4	13.4	-0.3

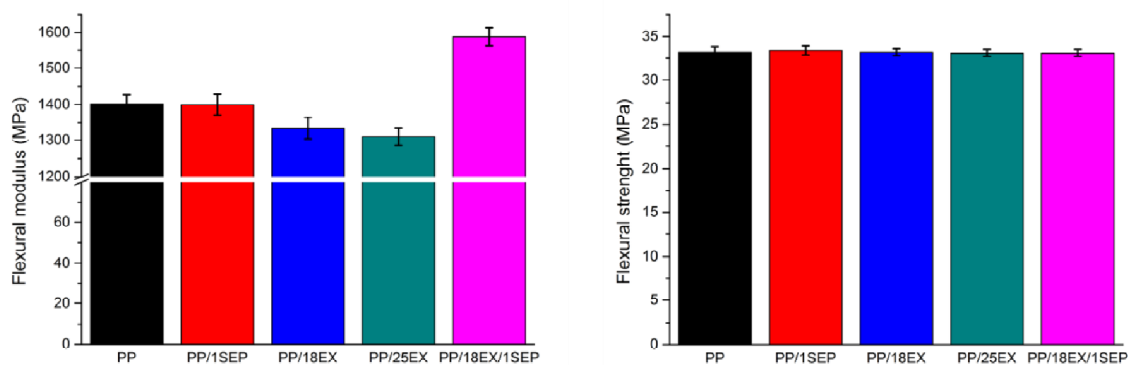


Figure 28. Flexural modulus and strength of the first set of materials.

4.5.2. Second set of materials

Adding 0.5 wt% SEP didn't change the mechanical properties of the matrix (Tab. 17). A small enhancement of the modulus was obtained by adding OSEP (+4%), probably because of the better arrangement of the macromolecules and the interactions with the surfactant used to modify the sepiolite. The small decrease of the flexural strength was negligible and, anyway, in the uncertainty range. Unlike the first set of materials, adding the flame retardant didn't worsen the flexural modulus of PP, as a matter of fact it allowed to achieve a small improvement of it (Fig. 29). On the other hand, the flexural strength of PP/12ET and PP/15ET was lower in comparison to the neat resin (respectively -16% and -21%).

With regard to the ternary formulations, the ET/SEP based formulation showed a small improvement of the modulus if compared to the binary formulations PP/0.5SEP and PP/12ET. The flexural strength was instead lower than that of PP and PP/0.5SEP but higher if compared to PP/12ET. This meant that SEP could somehow mitigate the negative effect due to the flame retardant. PP/12ET/0.5OSEP showed the highest modulus value (+10% in comparison to PP). The reason was connected with the high degree of crystallinity (41%) and the good affinity with the modified filler, inducing a more pronounced reinforcement effect of the matrix.

Table 17.
Mechanical properties of the second set of formulations.

	Flexural modulus (MPa)	Flexural strength (MPa)	Modulus variation (%)	Strength variation (%)
PP	1402 ± 25	33.2 ± 0.6	-	-
PP/0.5SEP	1420 ± 25	33.1 ± 0.3	1.4	-0.3
PP/0.5OSEP	1465 ± 15	32.8 ± 0.3	4.6	-1.2
PP/12ET	1440 ± 20	27.7 ± 0.2	2.8	-16.5
PP/15ET	1454 ± 20	26.1 ± 1.0	3.8	-21.4
PP/12ET/0.5SEP	1470 ± 30	28.5 ± 0.4	5.0	-14.1
PP/12ET/0.5OSEP	1532 ± 23	29.0 ± 1.0	9.4	-12.6

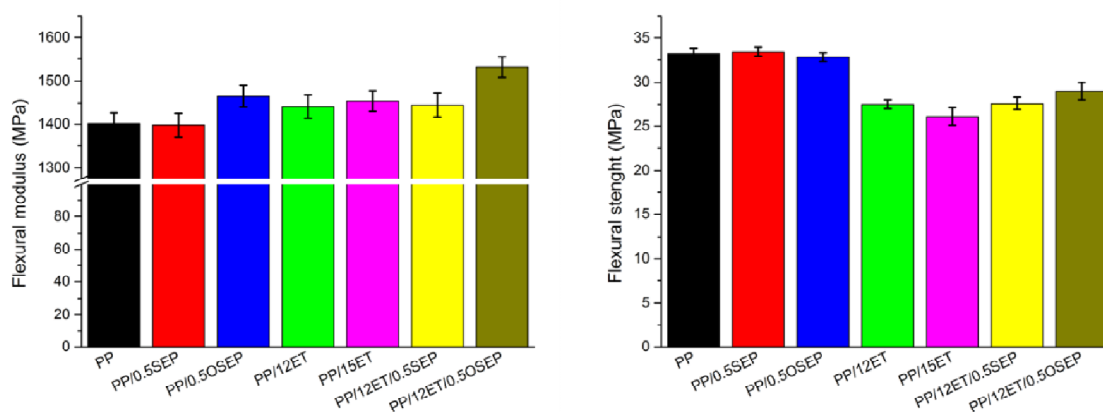


Figure 29. Flexural modulus and strength of the second set of materials.

Given that the only significant difference occurred between PP and the ET/OSEP based formulation, the Charpy impact tests were performed only for the above materials. The results confirmed what observed in the flexural tests. The load peak of PP/12ET/0.5OSEP was higher than that of PP, confirming the higher stiffness of the ternary composite. The resilience of the ternary system was instead lower if compared to the matrix. This suggested a worse ability to dissipate the impact energy (Fig. 30).

Table 18.
Impact properties of the second set of materials.

	Peak load (N)	Resilience (kJ/m ²)	Elongation at break (mm)
PP	216.6 ± 11.0	51.1 ± 6	6.8 ± 0.35
PP/12ET/0.5OSEP	246.2 ± 21.1	13.4 ± 2	3.6 ± 0.12

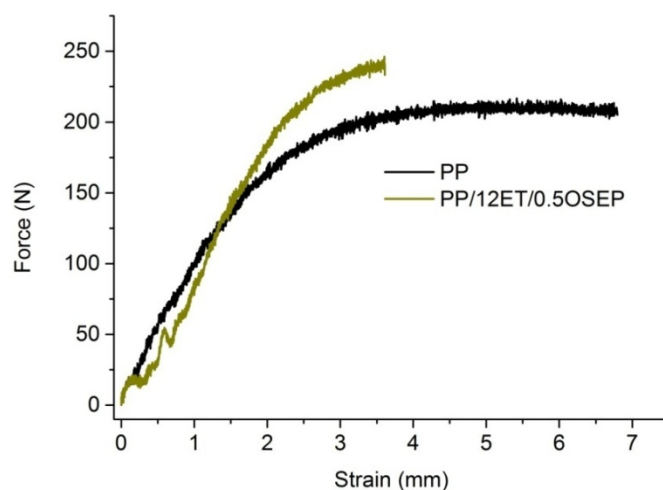


Figure 30. Outcomes of the impact tests.

4.6. Dynamic mechanical analysis (DMA)

4.6.1. First set of materials

Elastic modulus of the composites may be related to storage modulus obtained by dynamic mechanical analysis. The storage modulus curves as function of temperature are shown in Fig. 31.

Adding SEP induced a very limited effect on the properties of the matrix. Surprisingly, the inclusion of the flame retardant caused a pretty apparent improvement of the storage modulus of PP in the range 20 – 80 °C. The G' curve of the ternary formulation was clearly the most favorable in the range -50 – 60°C: this result is consistent with the flexural tests.

The tanδ curves showed that SEP didn't shifted the T_g of PP, so the nanofiller and the compatibiliser didn't have any influence on motion of the polymeric chains. Adding the flame retardant (18 or 25 wt%) made the T_g peak less noticeable (Fig. 32). The tanδ values of the EX based formulations were higher than those of the matrix in the range

60-120°C, leading to a less elastic behavior. The $\tan\delta$ curve of PP/18EX/1SEP resembled that of PP/18EX so the simultaneous presence of these two additives didn't lead to any further effect.

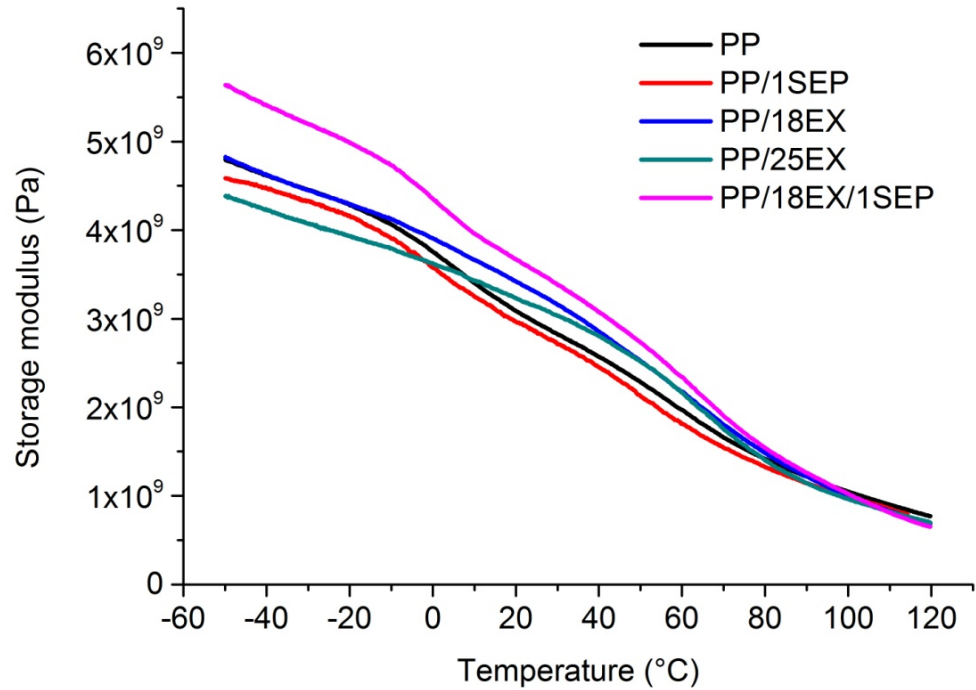


Figure 31. Storage modulus curves of the first set of materials.

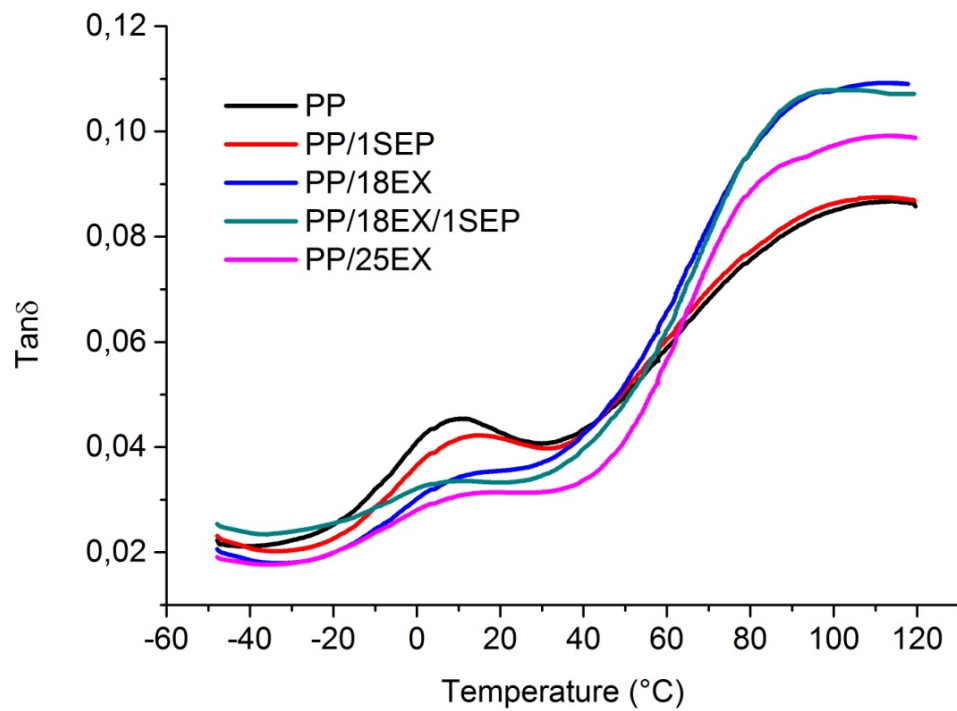


Figure 32. $\tan\delta$ curves of the first set of materials.

4.6.2. Second set of materials

The dynamic-mechanical analysis of the second set of materials reflected the flexural properties. It was seen that the addition of sepiolite particles did not induce any significant effect on the resin. The same result was observed after the addition of ET, 12 or 15 wt%. The presence of OSEP, instead, slightly improved the characteristics of PP in the temperature range $-50 - 60^{\circ}\text{C}$. The ternary formulation PP/12ET/0.5OSEP obtained good results as well: the storage modulus values were clearly higher than those of PP in the range from 0 to 120°C (Fig. 33).

The $\tan\delta$ curves showed that all formulations had almost the same trend, so the presence of flame retardant or nanofillers did not change either the T_g or the damping properties.

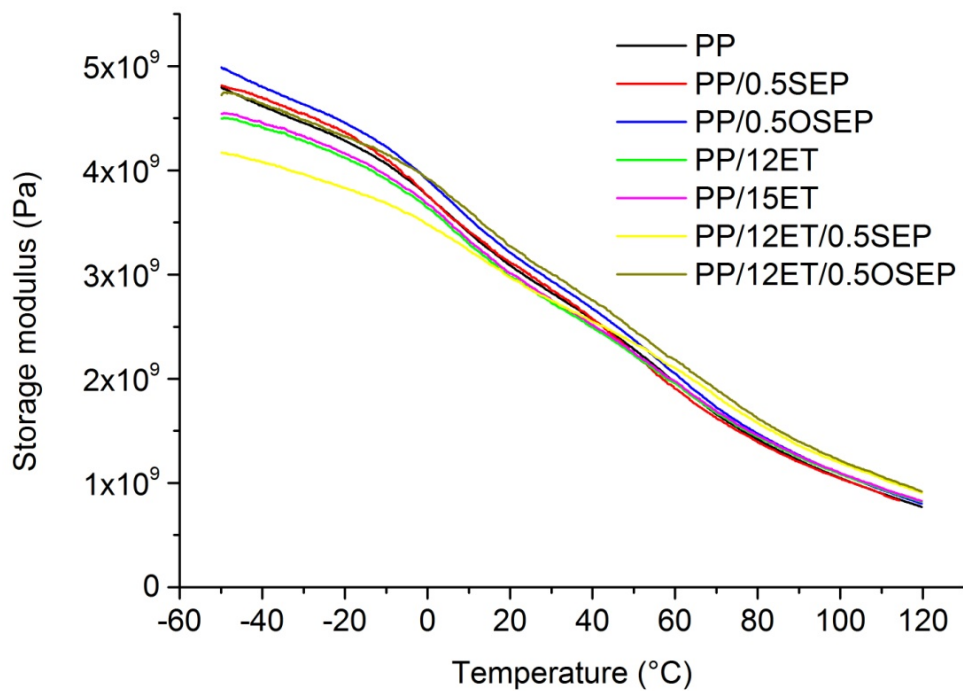


Figure 33. Storage modulus as function of temperature.

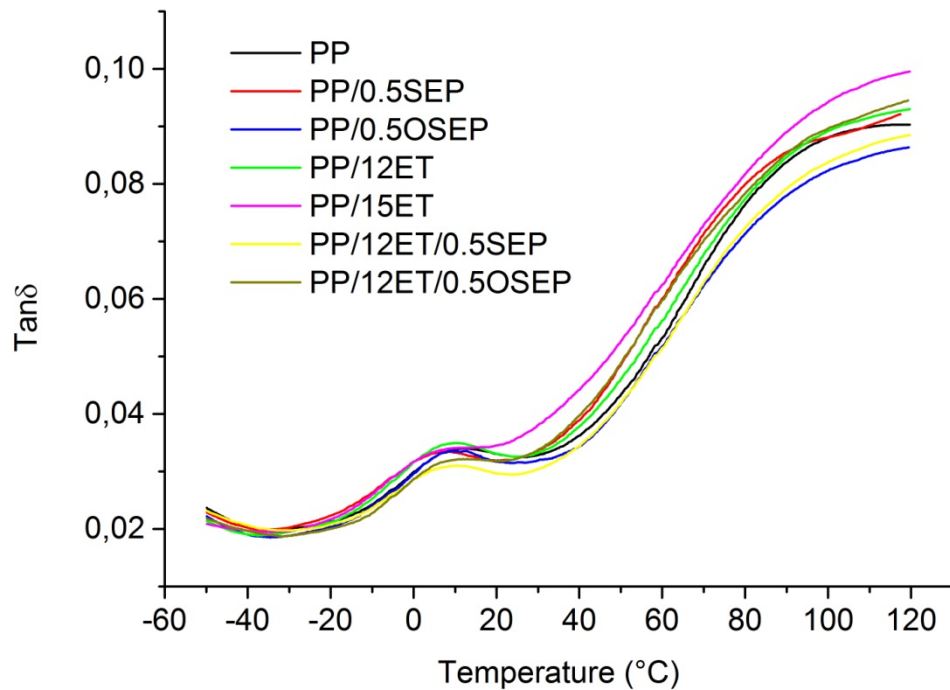


Figure 34. $\text{Tan}\delta$ as function of the temperature.

4.7. Rheological behavior

One of the aims of this chapter is to examine the effects of additives (flame retardants and nanoparticles) on the melt flow behavior of investigated formulations at high shear rates. This is an important aspect given that the melt viscosity is crucial for industrial processes: even if a material had excellent fire and mechanical properties but poor rheological properties, it would not be suitable for processes as injection molding, making all the effort useless.

The melt viscosity of both sets of materials was studied at high shear rates by using a capillary rheometer. With regard to the second set of materials, an additional study at low shear rates was performed to find any clues about the flammability properties.

4.7.1. First set of materials

The melt viscosity of PP/1SEP was a little lower than that of PP in the range 100-600 1/s, after that they were both identical. The reason was probably due to the easier motion of polymeric chains owing to the presence of the compatibiliser. The addition of 18 wt% EX led to an unusual result: at low shear rates, the viscosity was higher than that of PP but the opposite behavior was observed at high shear rates. The

addition of 25 wt% EX clearly increased the viscosity of the matrix in the range 1000-10000 1/s, so that percentage made the material not very suitable for processes such as injection molding. The curve of PP/18EX/1SEP showed that the presence of both fillers increased the melt viscosity of the material in all the used range (Fig. 35). The presence of the agglomerates observed by SEM analysis could explain such result: they likely made the motion and sliding of the polymeric chains more difficult to occur. This difference of viscosity was evident if compared to PP/18EX and PP, but it was acceptable considering the very good fire properties.

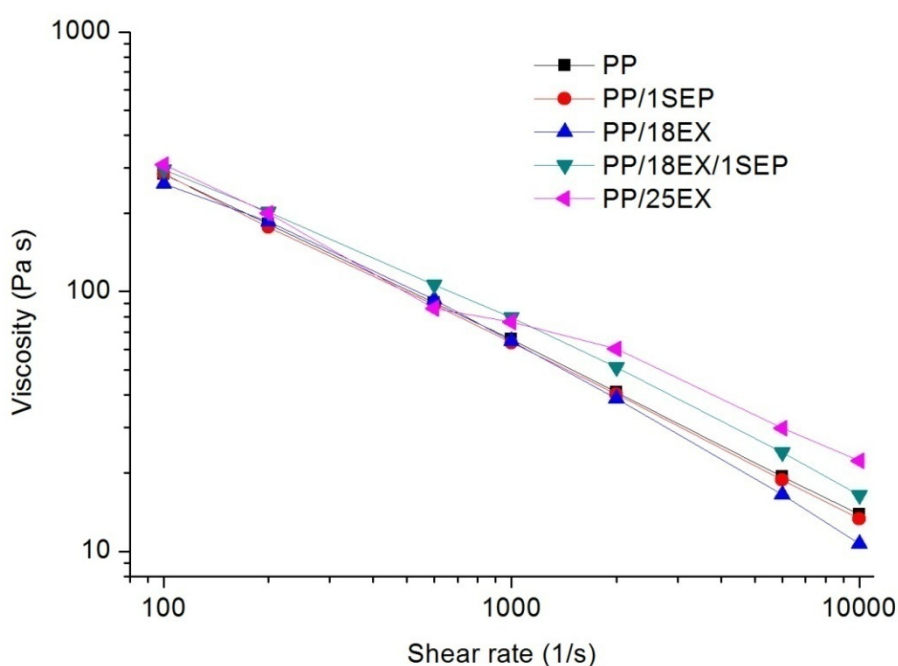


Figure 35. Melt viscosity of the first set of materials.

4.7.2. Second set of materials

The melt viscosity of PP/0.5SEP was a little lower than that of PP in the whole range of shear rates except for 10000 1/s, just as happened for PP/1SEP. This behavior was attributed to the presence of the compatibiliser. PP/0.5OSEP showed a pretty evident decrease of viscosity compared to PP, also at high shear rates (Fig. 36), owing to the organic surfactant inside the filler. Adding either 12 or 15 wt% ET didn't induce significant differences in comparison with PP. This was a confirm of the fine dispersion of the intumescent additive through the matrix. In the case of PP/12ET/0.5SEP, no particular effect was observed and the melt viscosity was the same of the corresponding

binary system, so the pristine nanofiller didn't play any role if mixed with the flame retardant. The same outcome was obtained if OSEP was used instead of SEP.

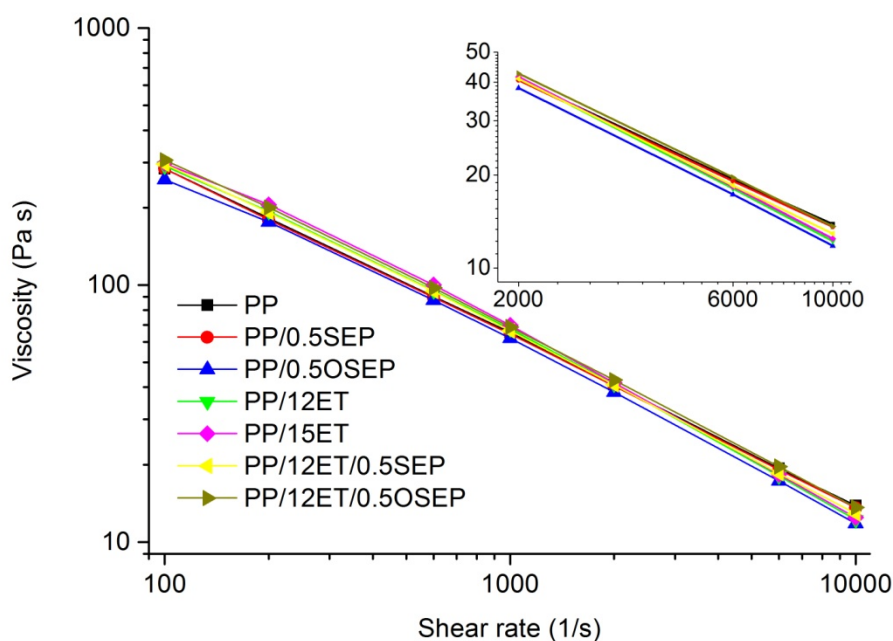


Figure 36. Melt viscosity at high shear rates.

With the aim to gain further insights about the flammability outcomes, in this case the rheological analysis was extended at low shear rates. The hypothesis was to justify the good flammability properties of PP/12ET/0.5OSEP with an increase of viscosity at low shear rates.

The neat matrix exhibited a classical shear thinning behavior. The inclusion of either 0.5 wt% SEP or OSEP increased the melt viscosity of PP over the entire frequency range examined (Fig. 37). Considering the very low amount of filler loading, the increase in viscosity is an indication of the achievements of a fine dispersion, much better if compared to an ordinary microcomposite. Adding 12 or 15 wt% of Exolit AP766 obviously increased the complex viscosity. Adding SEP or OSEP to PP/12ET barely shifted the viscosity curves of this binary formulation. Comparing the melt viscosity of PP/12ET with PP/12ET/SEP and PP/12ET/OSEP did not deliver any indication of improved flame retardancy, but was consistent with the similar intumescent behavior and fire residue observed for these materials.

Analyzing G' as a function of the shear rates can provide an indication about the degree of dispersion of the fillers. In the terminal region all the materials showed classical

viscous fluid behavior (Fig. 38). It was interesting to notice that OSEP nanoparticles increased the storage modulus more than that observed in the presence of SEP, confirming improved filler-matrix compatibility. Adding either 12 or 15 wt% of the intumescent substance provided a small increase in the modulus. It was noted that adding SEP or OSEP to the flame retardant led to opposite effects: the G' curve of PP/12ET/0.5SEP was less favorable than that of PP/12ET, but the ET/OSEP formulation showed higher G' values over the entire frequency range.

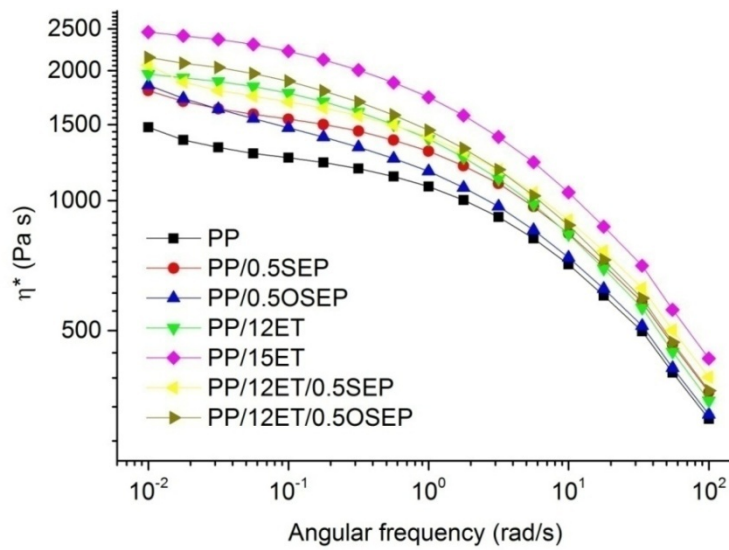


Figure 37. Complex viscosity as function of angular frequency.

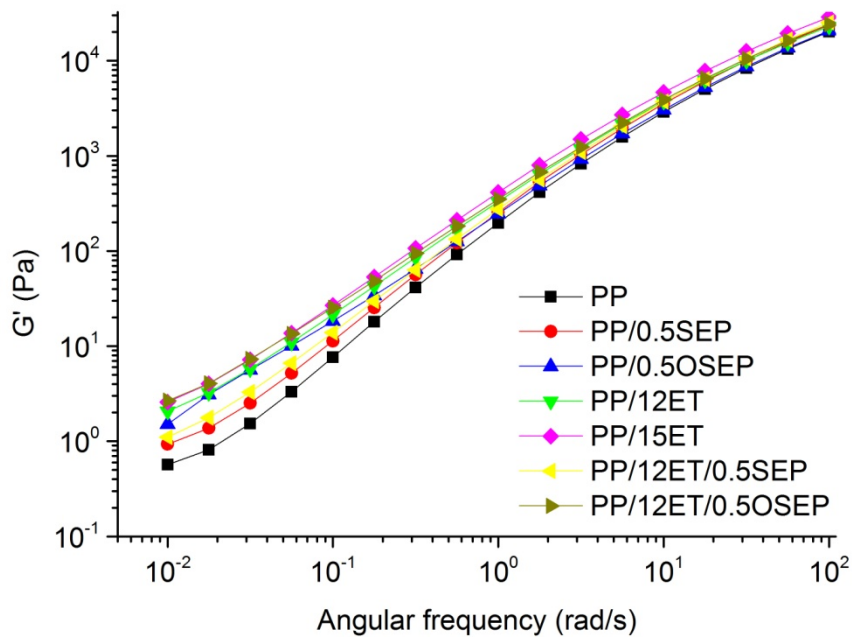


Figure 38. G' curves of the second set of materials.

4.8. Morphology of composites

4.8.1. First set of materials

SEM images of PP showed that the fracture surface was pretty smooth and free of significant defects (Fig. 39). Adding SEP didn't change the morphology, except for random light spots owing to nanometric agglomerates of the filler.

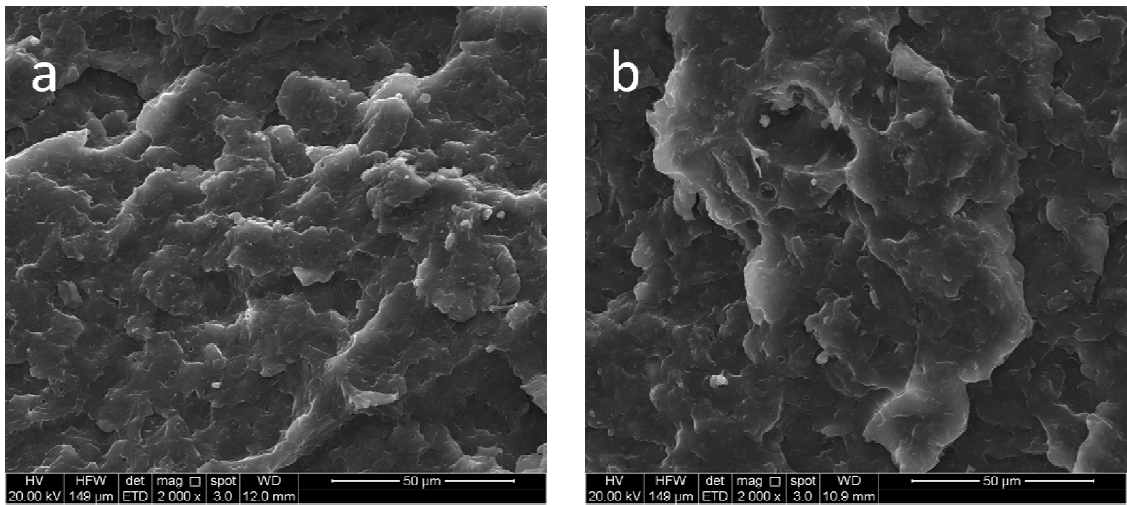


Figure 39. SEM micrographs of PP (a) and PP/1SEP (b) at 2000x magnification.

The fracture surface of PP/18EX didn't show any significant changes in comparison with PP (Fig. 40). At 2000x magnification, PP/18EX/1SEP looked like the binary formulation but an additional observation at higher magnification led to a surprising outcome: the surface was almost completely covered of small particles (Fig. 41), whose dimensions were around 100 nm. They were agglomerates involving flame retardant and sepiolite and surely represented a key factor to explain the very good fire properties obtained by cone calorimeter test.

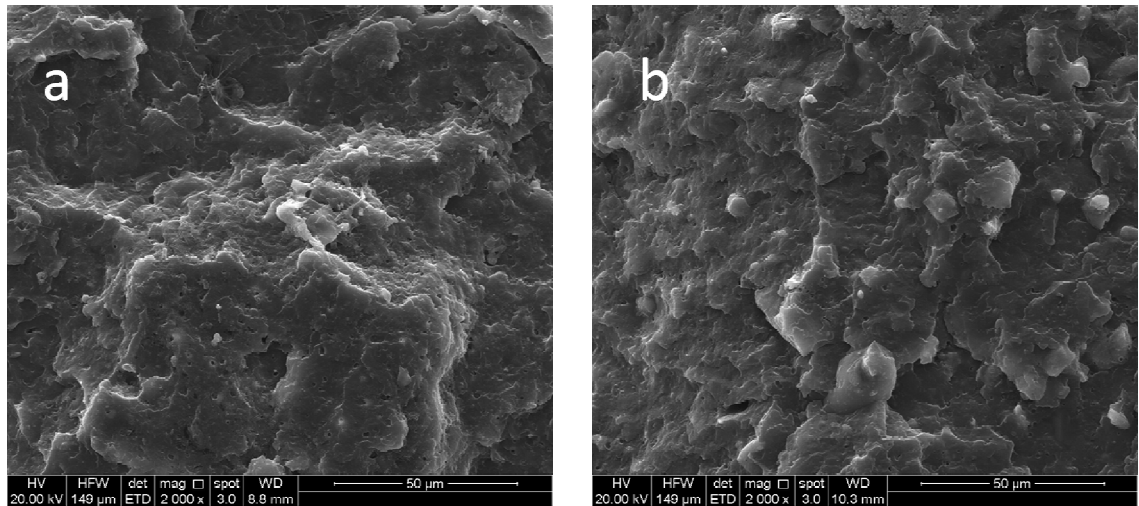


Figure 40. SEM micrographs of PP/18EX (a) and PP/18EX/1SEP (b) at 2000x magnification.

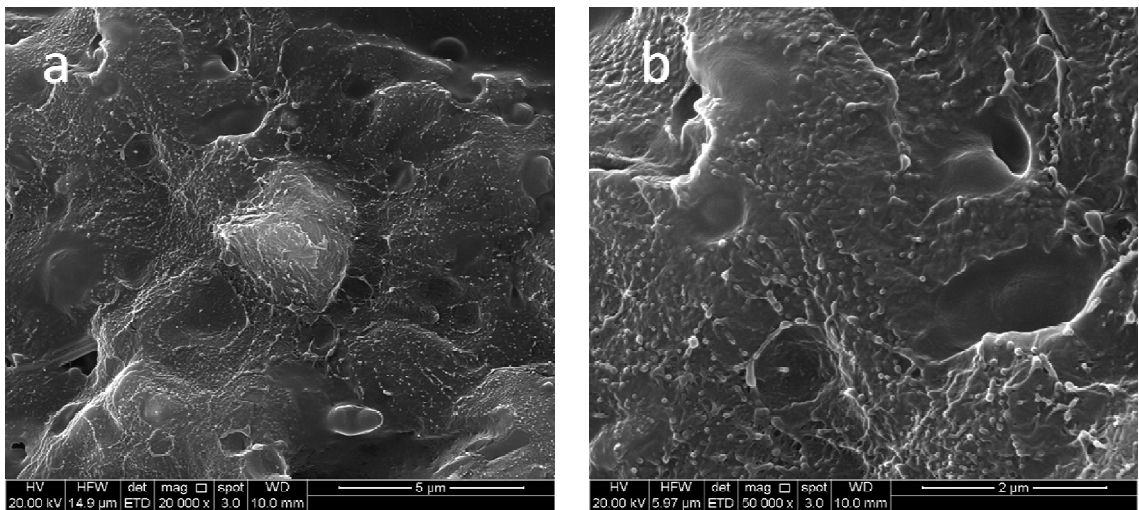


Figure 41. SEM micrographs of PP/18EX/1SEP at 20000x (a) and 50000x (b).

4.8.2. Second set of materials

Fig. 42 shows SEM micrographs of the materials containing SEP or OSEP at 500 and 5000x. There weren't any significant differences between the two formulations, also because of the very limited quantity of fillers contained inside the resin.

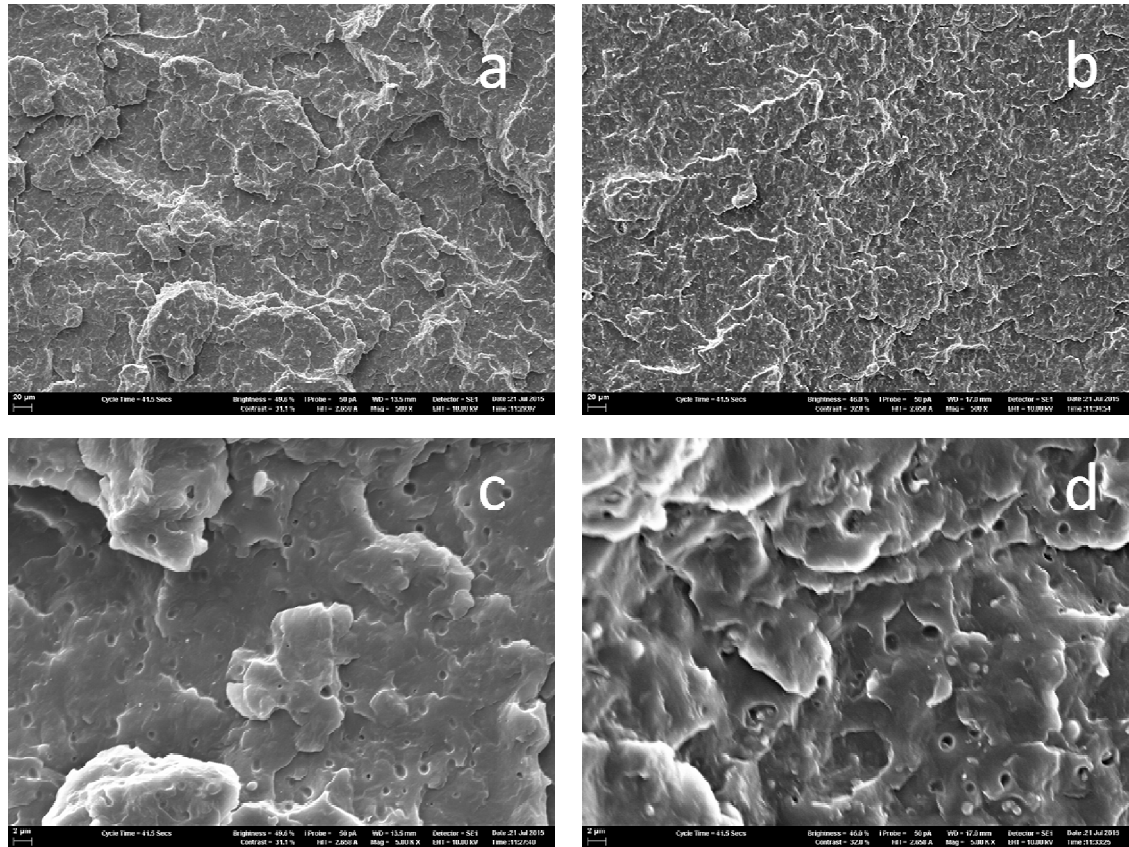


Figure 42. SEM micrographs of PP/0.5SEP (a, b); PP/0.5OSEP (c, d); upper images at 500x, lower images at 5000x.

Adding the flame retardant didn't change the morphology of the surface in evident way (Fig. 43). Such result was also due to the not excessive amount of Exolit AP 766. No significant changes were observed between the two formulations, despite of the different percentage of filler.

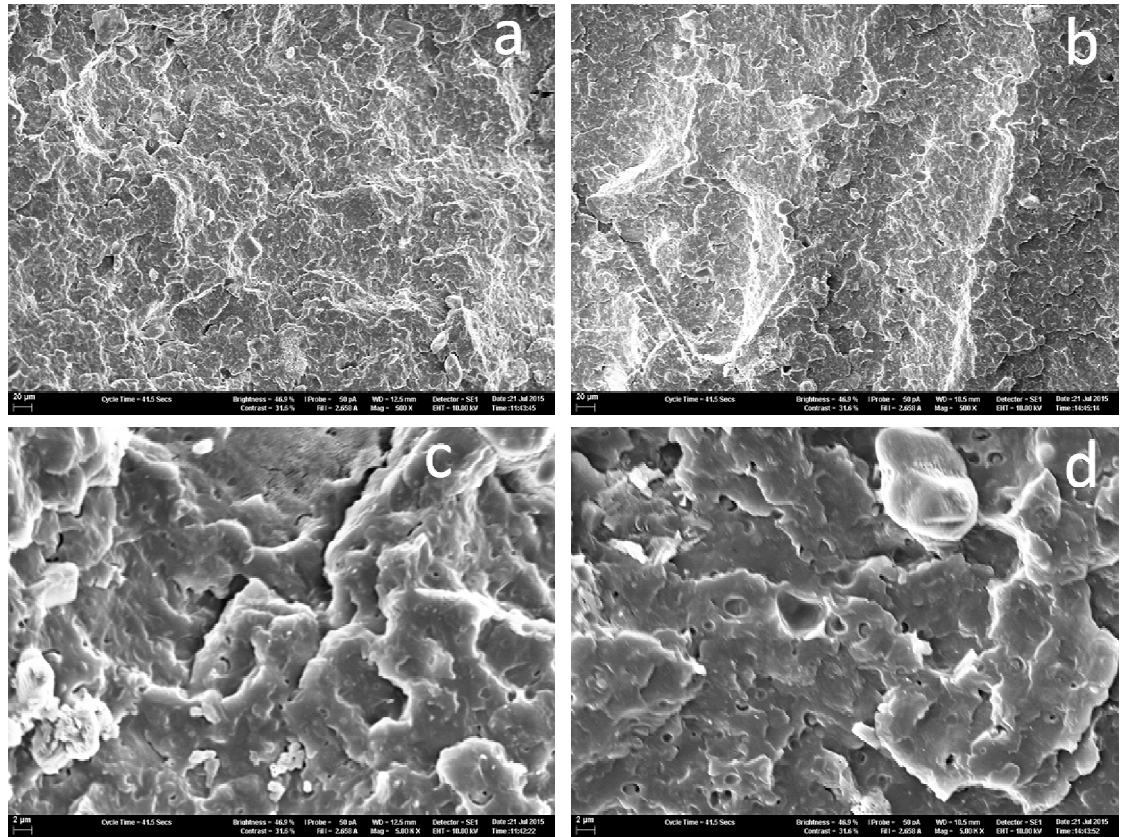


Figure 43. PP/12ET (a, b) and PP/15ET (c, d); Upper images taken at 500x, lower images taken at 5000x.

With regard to the ternary formulations, the pictures taken at 500x showed that the surface of PP/12ET/0.5OSEP was compact and almost free of significant flaws (Fig. 44) if compared to PP/12ET/0.5SEP. The micrographs at 5000x confirmed the above mentioned considerations.

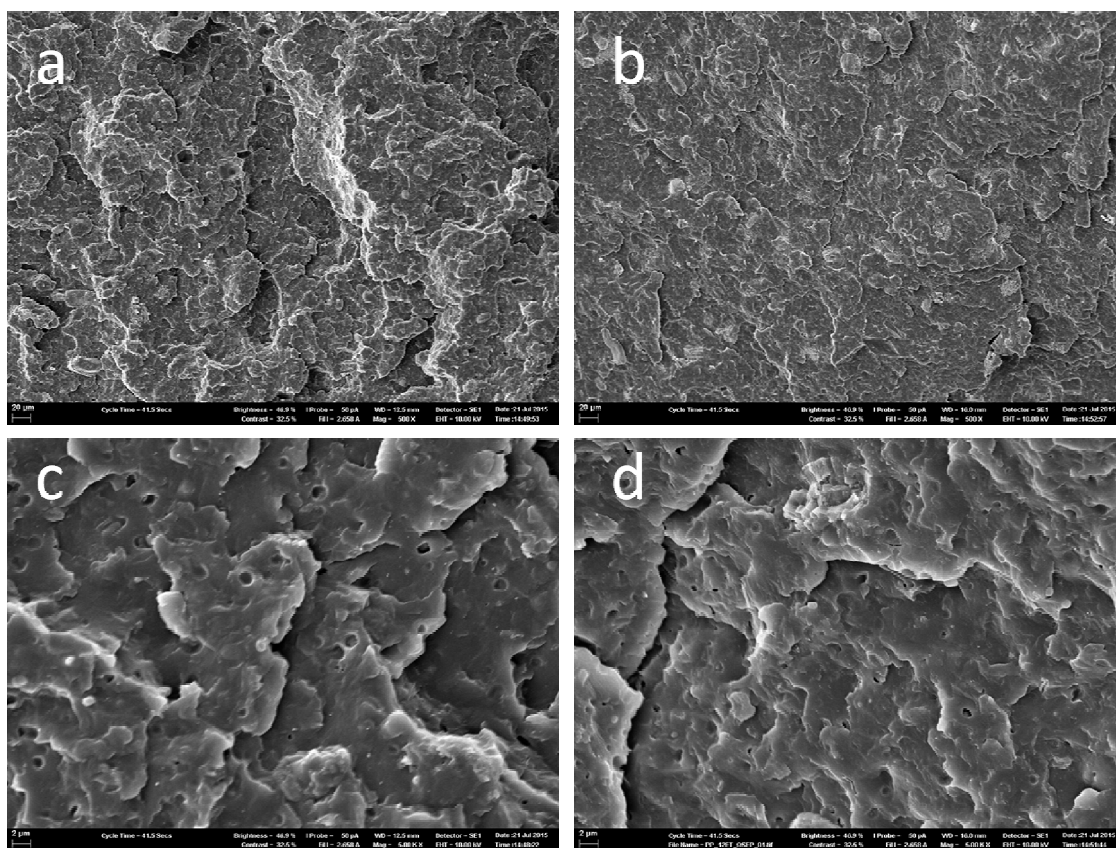


Figure 44. PP/12ET/0.5SEP at 500x and 5000x magnification (**a, b**); PP/12ET/0.5OSEP at 500x and 5000x magnification (**c, d**).

Fig. 45 shows SEM micrographs of the fire residue surface of the materials. All of them showed similar structure on the microscopic scale. The surface of the residues was a very compact structure with only a few holes and cracks. This feature was surely the reason of the large protective layer effect observed during the cone calorimeter analysis. At larger magnification (Fig. 46) it was possible to notice interesting differences. Different agglomerates became visible: a number of sepiolite nanoparticles, which probably appeared on the surface during the combustion test, were evident in the ternary systems and gave rise to more rugged surface in the case of ET/OSEP based formulation. This feature could be related to the different fire performances but wasn't enough to explain such characteristics.

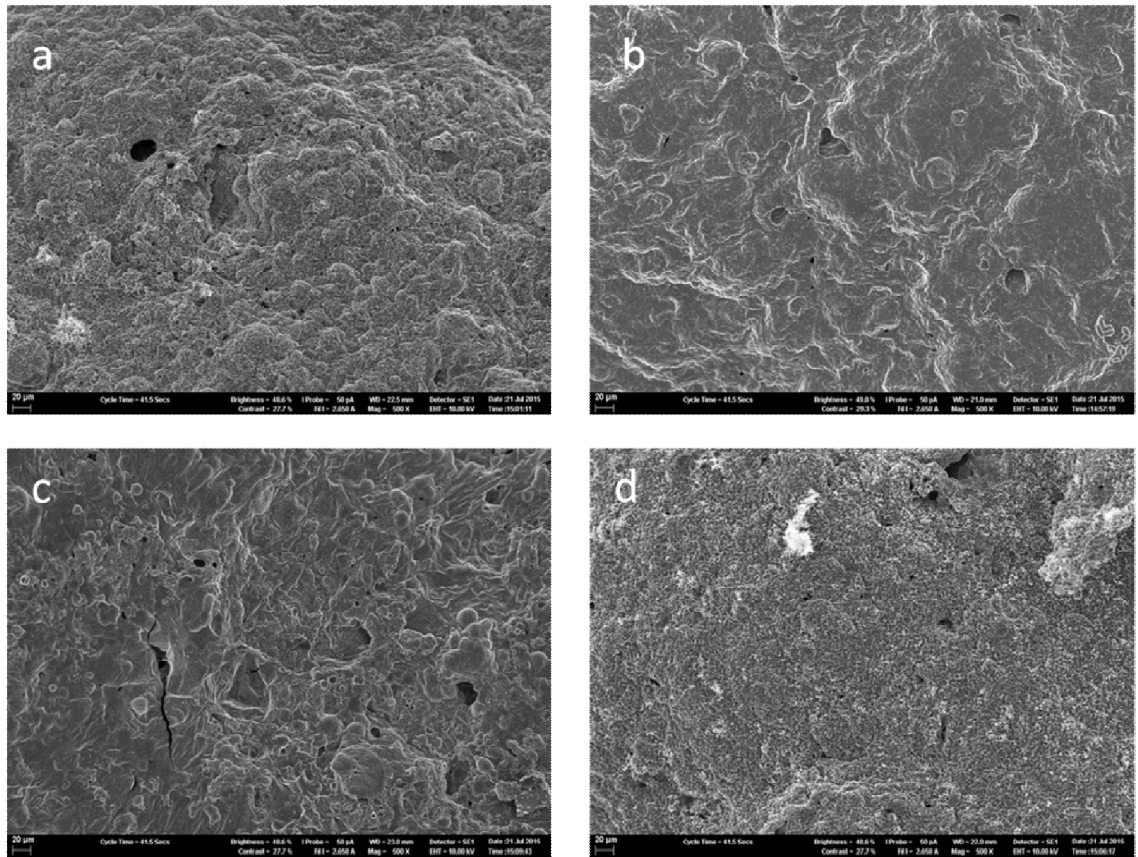


Figure 45. SEM micrographs of the cone residues: PP/12ET (a), PP/15ET (b), PP/12ET/0.5SEP (c), PP/12ET/0.5OSEP (d); 500x.

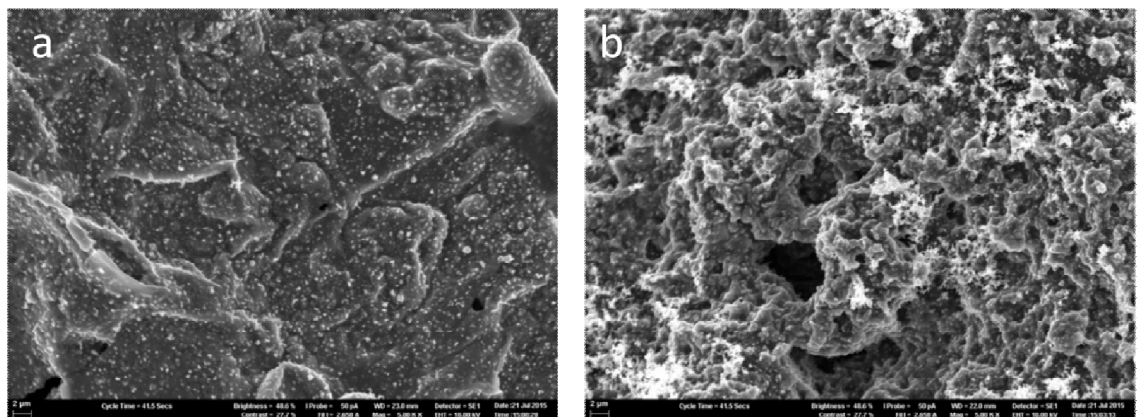


Figure 46. SEM micrographs of PP/12ET/0.5SEP (a) and PP/12ET/0.5OSEP (b); 5000x magnification.

TEM micrographs of PP/0.5SEP showed that the nanofiller was not uniformly dispersed as exfoliated particles in the matrix but agglomerates 300–700 nm in size were observed and there was a lack of separated single particles (Fig. 47). PP/0.5OSEP samples showed a morphology similar to that of PP/0.5SEP, despite the presence of the surfactant used to modify the nanofiller. As a consequence, these two binary

formulations may be classified as on the border between very fine microcomposites and real nanocomposites. This lack of dispersion was supposed to explain the very limited effect of these nanofillers in PP/SEP and PP/OSEP materials.

With regard to the ternary systems, there was a significant difference: the ET/OSEP formulation showed much better filler dispersion if compared to the ET/SEP one (Fig. 48). Such result was consistent with the improved flammability and fire properties detected for this material.

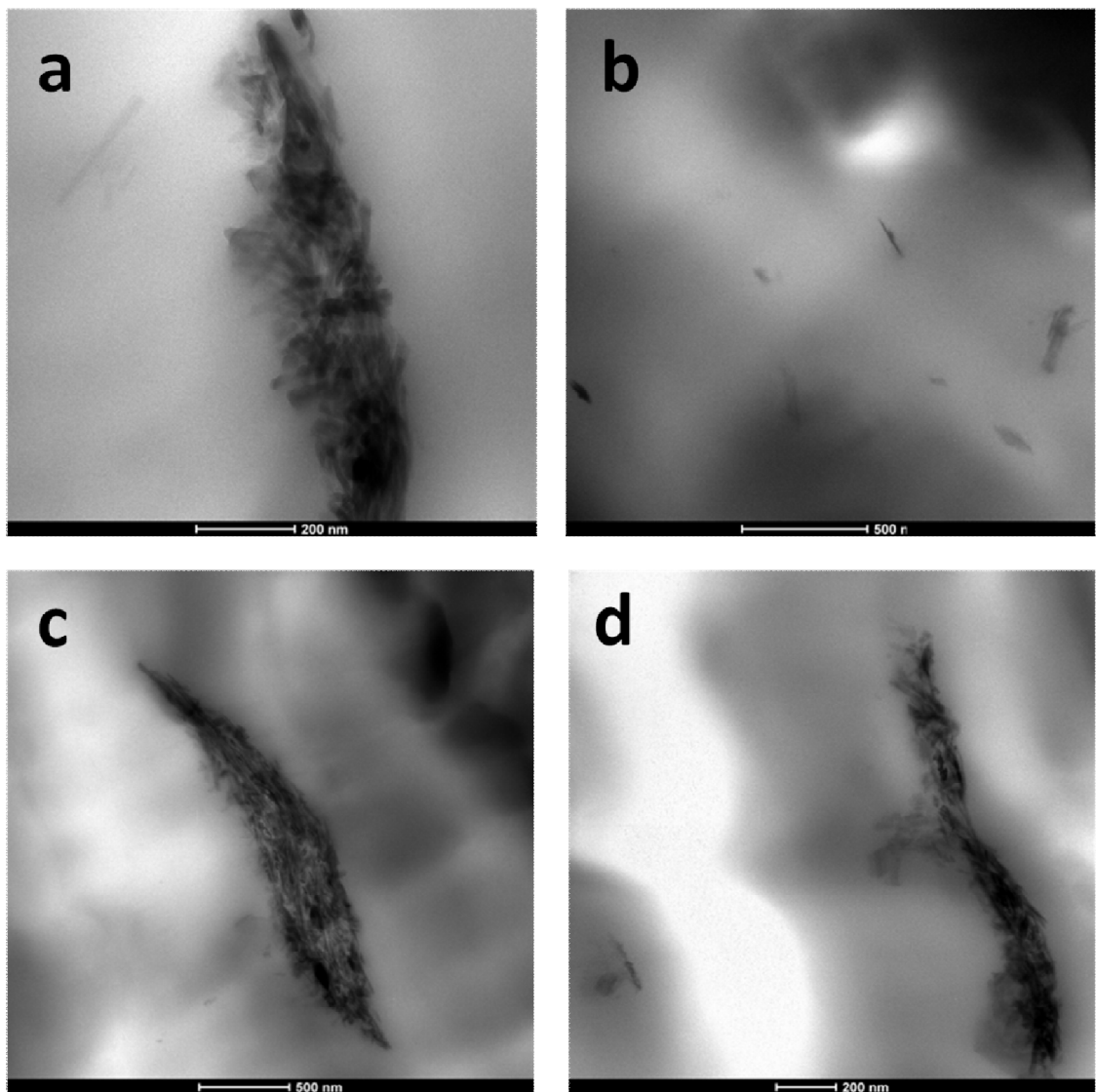


Figure 47. TEM micrographs of PP/0.5SEP (a, b) and PP/0.5OSEP (c, d).

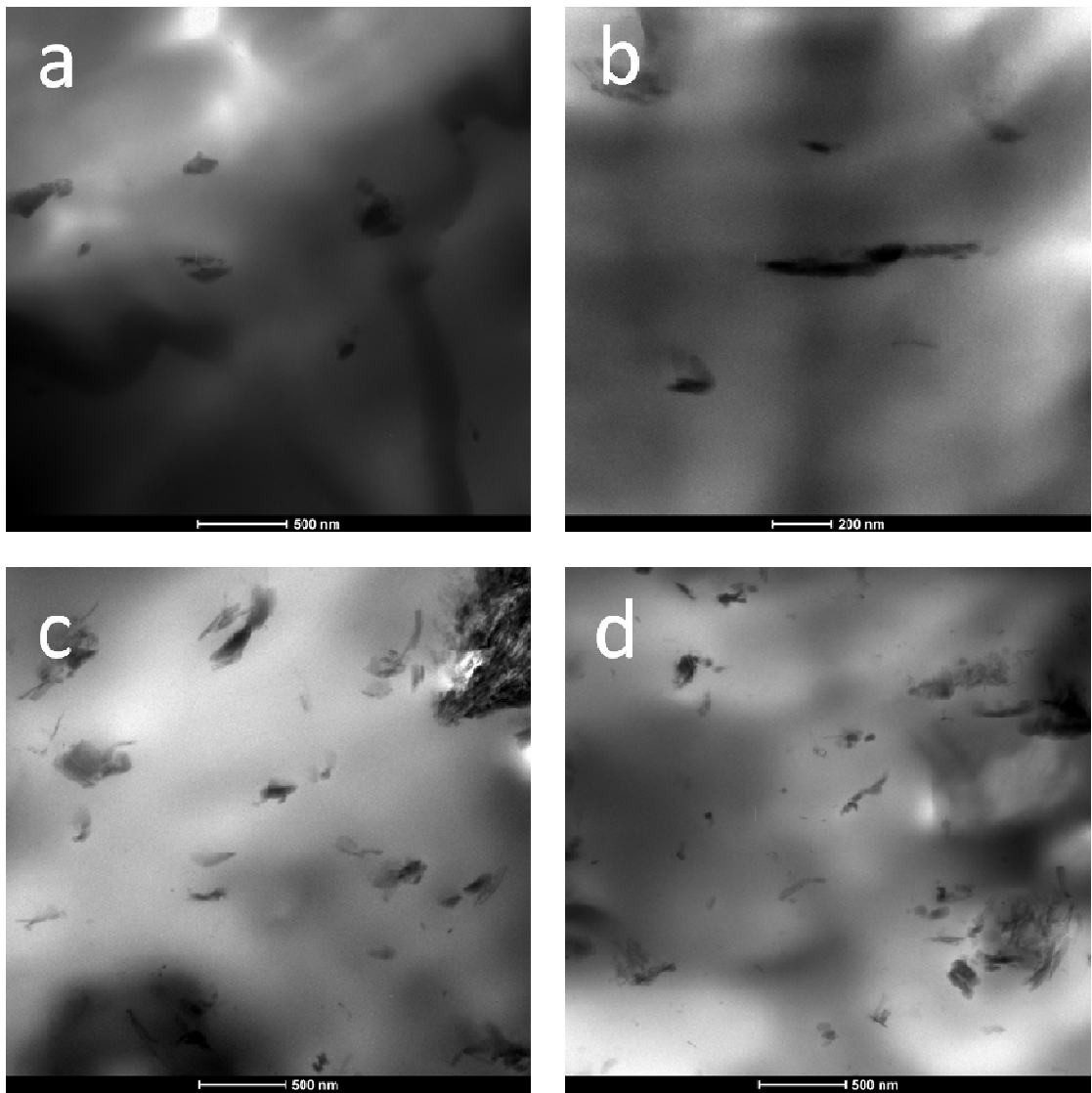


Figure 48. TEM micrographs of PP/12ET/0.5SEP (a, b) and PP/12ET/0.5OSEP (c, d).

4.9. Conclusions

In this work the thermal, fire, mechanical and rheological properties of two sets of polypropylene based compounds filled with intumescent substances and sepiolite, either pristine or modified, were investigated. The thermal behavior was analyzed by thermogravimetry, the fire behavior was observed by flammability tests and cone calorimeter measurements. The melt viscosity, at high or low shear rates, allowed to study the processability of the investigated formulation and the degree of dispersion of the additives. The mechanical tests instead highlighted the effect of the fillers on the flexural and impact properties.

About the first set of materials, the TGA showed that the addition of sepiolite coupled with Exolit AP750 could improve the thermal stability of PP, as pointed out by the lower mass loss rate and increased residue yield. Pristine sepiolite alone slightly worsened the flammability properties of the resin but, when coupled with Exolit AP750, gave rise to a synergic effect for the fire behavior. The forced combustion analysis confirmed what written above: all the main parameters, such as HRR, THR and TSP, highlighted a fire behavior very similar between PP/25EX and PP/18EX/1SEP. The flexural tests showed that the simultaneous presence of sepiolite and flame retardant enhanced the modulus (+13.4% compared to PP). The dynamic mechanical analysis results were in accordance with the flexural properties. With regard to the rheological behavior at high shear rates, the melt viscosity of PP/18EX/1SEP was lower than that of PP/25EX but still higher in comparison to the resin. Anyway this feature was not a serious drawback if the good fire properties of the ternary formulation are taken into account. The existence of many nanometric agglomerates of sepiolite and flame retardant (observed by SEM) was most likely a key factor for the fire and mechanical properties.

The characterization of the second set of materials pointed out the synergic effect between organically modified sepiolite and Exolit AP766. The UL-94, LOI and cone calorimeter tests showed that 0.5 wt% OSEP could boost the efficiency of the flame retardant: the flammability and fire properties of PP/12ET/0.5OSEP were even better than those of PP/15ET, despite the lower amount of ET used. This result was due to the formation of a very effective char layer at high temperatures which prevents the oxygen and heat exchange. The flexural and impact tests proved that OSEP, thanks to the high compatibility with the resin, could improve the mechanical behavior of PP. The rheological and morphological analysis showed that OSEP was very well dispersed throughout the matrix, providing an addition explanation of the good fire properties despite the low amount used.

Overall, this research work has shown the effectiveness of sepiolite as synergic agents for flame retardants. Particularly, the very good dispersion of small percentages of OSEP seems to be promising in terms of fire behavior, allowing to reduce the amount of flame retardant normally required to achieve a good fire safety.

References

1. Demir H., Arkis E., Ulku S. Synergistic effect of natural zeolites on flame retardant additives. *Polym. Degrad. Stab.* 2005; 89: 478-83.
2. Bourbigot S., Le Bras M., Delobel R., Breant P., Tremillon J-M. 4A zeolite synergistic agent in new flame retardant intumescent formulations of polyethylenic polymers - study of the effect of the constituent monomers. *Polym. Degrad. Stab.* 1996; 54: 275-87.
3. Ravadits I., Toth A., Marosi G., Marton A., Szep A. Organosilicon surface layer on polyolefins to achieve improved flame retardancy through an oxygen barrier effect. *Polym. Degrad. Stab.* 2001; 74: 419-22.
4. Marosi G., Marton A., Anna P., Bertalan G., Marosfoi B., Szep A. Ceramic precursor in flame retardant systems. *Polym. Degrad. Stab.* 2002; 77: 259-65.
5. Estevao L.R.M., Le Bras M., Delobel R., Nascimento R.S.V. Spent refinery catalyst as a synergistic agent in intumescent formulations: influence of the catalyst's particle size and constituents. *Polym. Degrad. Stab.* 2005; 88: 444-55.
6. Wu Qiang, Qu Baojun. Synergistic effects of silicotungstic acid on intumescent flame retardant polypropylene. *Polym. Degrad. Stab.* 2001; 74: 255-61.
7. Liu Yuan, Wang Qi. Catalytic action of phospho-tungstic acid in the synthesis of melamine salts of pentaerythritol phosphate and their synergistic effects in flame retarded polypropylene. *Polym. Degrad. Stab.* 2006; 91: 2513-9.
8. M. He, W. C. Cao, L. J. Wangb, C. A. Wilkie Synergistic effects of organo-sepiolite and zinc borate on the fire retardancy of polypropylene. *Polymers for Advanced Technologies* Volume 24, Issue 12, pages 1081–1088, December 2013
9. N. H. Huang, Z. J. Chen, J. Q. Wang, P. Wei, *eXPRESS Polymer Letters* Vol.4, No.12 (2010) 743–752.
10. United Kingdom Fire Statistics 2004, Home Office, London, 2006.
11. M. Rigolo, R. T. Woodhams. *Poly. Eng. Sci.* 32 (1992) 327.
12. L. Haurie, A .I. Fernandez, J. I. Velasco, J. M. Chimenos, J.-M. Lopez-Cuesta, F. Espiell, *Polym. Degrad. Stab.* 91 (2006) 989.
13. ISO 19706:2007 Guidelines for assessing the fire threat to people.
14. G. Pal, H. Macskasy, *Plastics: Their behavior in fires*, Elsevier, New York, (1991)

15. NFX 70-100, Analysis of pyrolysis and combustion gases. Tube furnace method. Part 1, Methods of analysis of gas generated by thermal degradation. Part 2, Method of thermal degradation using tube furnace.
16. ISO 5659-2:1999 Plastics-Smoke Generation-Part 2, Determination of Specific Optical Density.
17. K. Shen K., *Plastics Compounding*, Nov/Dec (1988) 26
18. M. S. Cross, P. A. Cusack, P. R. Hornsby, *Polym. Degrad. Stab.* 79 (2003) 309
19. S. Utamapanya, K. J. Klabunde, J.R. Schlup. *Chem. Mater.* 3 (1991) 175
20. Y. Ding, G. Zhang, H. Wu, B. Hai, L. Wang, Y. Qian, *Chem. Mater.* 13 (2001) 435
21. C. Henrist, J.-P. Mathieu, C. Vogels, A. Rulmont, R. Cloots, *J. Cryst. Growth.* 249 (2003) 321
22. L. Qiu, R. Xie, P. Ding, B. Qu, *Compos. Struct.* 62 (2003) 391
23. L. Delfosse, C. Baillet, A. Brault, D. Brault, *Polym. Degrad. Stab.* 23 (1989) 337
24. E. D. Weil, *Encyclopedia of Polymer Science and Technology*. Wiley Interscience, New York, 11 (1986)
25. A. M. Aronson, *Phosphorous Chemistry*, ACS Symposium, 486 (1992) 218
26. J. Davis, M. Huggard, *J. Vinyl. Addit. Technol.* 2 (1996) 69
27. Y. F. Shih, Y. T. Wang, R. J. Jeng, K. M. Wei, *Polym. Degrad. Stab.* 86 (2004) 339
28. S. V. Levchik, L. Costa and G. Camino, *Polym. Degrad. Stab.* 43 (1996) 43
29. S; Duquesne, M. Le Bras, S. Bourbigot, R. Delobel, G. Camino, B. Eling, C. Lindsay, T. Roels, H. Vezin, *J. Appl. Polym. Sci.* 82 (2001) 3262
30. S. V. Levchik, D. A. Bright, G. R. Alessio, S. Dashevsky, *J. Vinyl. Addit. Technol.* 7 (2001) 98
31. S. V. Levchik, D. A. Bright, P. Moy, S. Dashevsky, *J. Vinyl. Addit. Technol.* 6 (2000) 123
32. S. V. Levchik, D. Weil, *Polym. Int.* 54 (2005) 11
33. L. Costa, G. Camino, D. Luda, P. Cortemiglia, *Fire and Polymers*, ACS Symposium, Washington DC, 425 (1990) 211
34. T. Kashiwagi, J. W. Gilman, *Fire retardancy of polymeric materials*, Marcel Dekker Inc., New York, A. F. Grand and C. A. Wilkie Editors, 10 (2000) 353
35. W. Zhou, H. Yang, *Thermochim. Acta.* 452 (2007) 43
36. J. W. Gilman, T. Kashiwagi, R. H. Harris Jr, S. Lomakin, J. D. Lichtenhan, P. Jones, A. Bolf. In : S. Al-Malaika, C. Wilkie, C.A Golovoy, eds. *Chemistry and Technology of Polymer Additives*. London: Blackwell Science, (1999) 135

37. M. Zanetti, T. Kashiwagi, L. Falqui, G. Camino, *Chem. Mater.* 14 (2002) 881
38. M. Lewin, *Polym. Adv. Technol.* 17 (2006) 758
39. S. Peeterbroeck, F. Laoutid, J.-M. Taulemesse, F. Monteverde, J.-M. Lopez-Cuesta, J. B. Nagy, M. Alexandre, Ph. Dubois, *Adv. Funct. Mater.* 17 (2007) 2787
40. Z., Jin K. P.Pramoda, G. Xu, S. H.Goh, *Chem. Phys. Lett.* 337 (2001) 43
41. C. A.Cooper, D. Ravich, D. Lips, J. Mayer, H. D.Wagner, *Compos. Sci. Technol.* 62 (2002) 1105 70
42. [33] B. H. Cipiriano, T. Kashiwagi, S. R. Raghavan, Y. Yang, E. A. Grulke, K. Yamamoto, J. R. Shields, J. F. Douglas, *Polym.* 48 (2007) 6086
43. T. Kashiwagi, F. Du, K. I. Winey, K. M. Groth, J. R. Shields, S. P. Bellayer, H. Kim, J. F. Douglas, *Polym.* 46 (2005) 471
44. B. Schartel, P. Potschke, U. Knoll, M. Abdel-Goad. *Eur. Polym. J.* 41 (2005) 1061
45. S. Bocchini, A. Frache, G. Camino, M.Claes, *Eur. Polym. J.* 43 (2007) 3222
46. M.R. Weir, W. Kuang, G.A. Facey, C. Detellier, *Clays Clay Miner.* 50 (2002) 240.
47. G. Sandi, R.E. Winans, S. Seifert, K.A. Carrado, *Chem. Mater.* 14 (2002) 739.
48. W. Kuang, G.A. Facey, C. Detellier, B. Casal, J.M. Serratos, E. Ruiz-Hitzky, *Chem. Mater.* 15 (2003) 4956.
49. D.A. McKeown, J.E. Post, E.S. Etz, *Clays Clay Miner.* 50 (2002) 667.
50. R.L. Frost, Z. Ding, *Thermochimica Acta* 397 (2003) 119.
51. C.R. Herrero, E. Morales, J.L. Acosta, *Die Angewandte Makromolekulare Chemie* 205 (1993) 97.
52. C.R. Herrero, E. Morales, J.L. Acosta, *J. Appl. Polym. Sci.* 51 (1994) 1189.
53. J.L. Acosta, C.R. Herrero, E. Morales, *Die Angewandte Makromolekulare Chemie* 175 (1990) 129.
54. J.L. Acosta, L. Gonza`lez, M.C. Ojeda, C. Del Ri`o, *J. Appl. Polym. Sci.* 86 (2002) 3512.
55. L. Bokobza, A. Burr, G. Garnaud, M.Y. Perrin, S. Pagnotta, *Polym. Int.* 53 (2004) 1060.
56. L. Bokobza, J.-P. Chauvin, *Polymer* 46 (2005) 4144.
57. L. Gonzalez, A. Rodriguez, A. Marcos-Fernandez, A. Del Campo, *J. Appl. Polym. Sci.* 79 (2001) 714.
58. N. H. Huang, Z. J. Chen, J. Q. Wang, P. Wei, *eXPRESS Polymer Letters* Vol.4, No.12 (2010) 743–752.

59. M. He, W. C. Cao, L. J. Wang, C. A. Wilkie, *Polym. Adv. Technol.* 2013, 24 1081–1088.
60. Antonov, M. Yablokova, L. Costa, A. Balavanovich, G. Levchik, S. Levchick, *Mol. Cryst. Liq. Cryst. Sci. Technol. Sect. A* 353 (2000) 203
61. A. Fina, D. Tabuani, A. Frache, G. Camino, *Polym.* 46 (2005) 7855
62. A. Fina, H. C. L. Abbenhuis, D. Tabuan, G. Camino, *Polym. Degrad. Stab.* 91 (2006) 2275
63. A. Fina, H. C. L. Abbenhuis, D. Tabuani, A. Frache, G. Camino, *Polym. Degrad. Stab.* 91 (2006) 1064
64. G. Tartaglione, D. Tabuani, G. Camino, *Microporous and Mesoporous Materials* 107 (2008) 161–168
65. Gensler R., Plummer C.J.G., Kausch H., Kramer E., Pauquet J.R., Zweifel H. Thermo-oxidative degradation of isotactic polypropylene at high temperatures: phenolic antioxidants versus HAS. *Polym Degrad Stab* 2000;67:195e208.
66. F. Samyn, S. Bourbigot, S. Duquesne, R. Delobel, *Thermochimica Acta* Volume 456, Issue 2, 15 May 2007, Pages 134–144
67. Horrocks A.R., Smart G., Nazare S., Kandola B., Price D., Quantification of zinc hydroxystannate and stannate synergies in halogen-containing flame retardant polymeric formulations. *J. Fire Sci.* 2010; 28:217-248.

Acknowledgments

Ed eccoci alla parte più difficile da scrivere, dato che si rischia sempre di scontentare qualcuno...Il mio primo pensiero va alla mia famiglia, che mi ha sempre supportato e dato buoni consigli nei momenti di difficoltà.

Desidero ringraziare i professori Acierno e Russo per la possibilità di intraprendere e portare a termine questo percorso formativo, fonte di tante soddisfazioni. Un caloroso pensiero va a Bernhard Schartel, sempre pronto a darmi ogni spiegazione richiesta, ed al suo gruppo di ricerca del BAM. Nonostante abbia trascorso solo tre mesi a Berlino, è stato un bellissimo periodo, in cui ho lavorato con proficiuità e conosciuto tante persone di nazionalità differenti.

Passando ai miei colleghi, il primo pensiero va a Vincenzo che mi ha sempre aiutato con estrusioni e prove reologiche, permettendomi di finire ogni lavoro in poco tempo. Come dimenticare di Antonella, che mi ha concesso l'onore di sedere al suo fianco per tre anni, anche se in uno spazio limitato...Un sincero ringraziamento anche a Giorgio, che mi ha sempre dato utili consigli, non solo in merito al dottorato. Desidero quindi ringraziare tutti i miei colleghi del dipartimento, in particolare Adolfo, Francesco e Lucia che non hanno mai negato il loro aiuto. Infine un caloroso ringraziamento a Paola Desidery, che mi ha sempre aiutato a uscire indenne da montagne di certificati, domande e carte bollate.

Non so cosa mi riserverà il futuro ma una cosa è certa, porterò sempre con me il ricordo di questi tre anni trascorsi al DICMAPI. Le giornate passate in laboratorio, le relazioni da finire in tempo, le chiacchierate con gli amici, le pause-pranzo e caffè...non dimenticherò nulla di tutto questo. Grazie di cuore a tutti.